ACS OMEGA

Open Access

http://pubs.acs.org/journal/acsodf

Article

Mineralogy and Geochemistry of Rare Earth Elements in Carboniferous-Permian Coals at the Eastern Margin of the Ordos Basin

Long Wen, Wenhui Huang,* Yuanfu Zhang,* Bo Jiu, Deyu Yan, Ruilin Hao, and Huidi Hao

Cite This: *ACS Omega* 2024, 9, 32481−32501

Read Online

ACCESS | Metrics & More | Article Recommendations

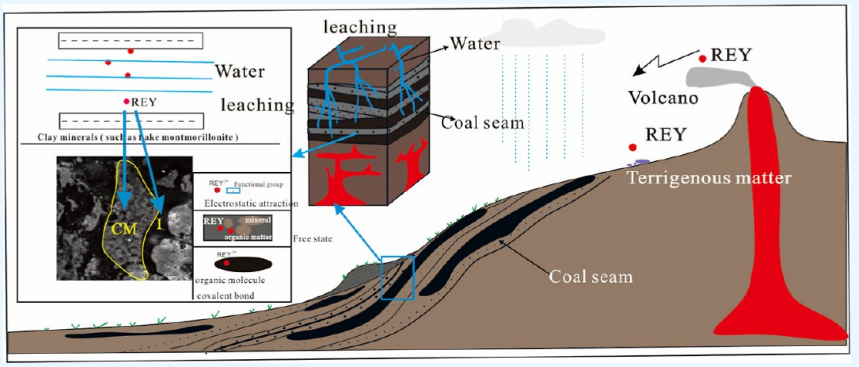

ABSTRACT: This article used Carboniferous-Permian coals from the Jungar, Hedong, and Weibei Coalfields in the east of the Ordos Basin as research samples. Characteristics of coal quality, petrology, mineralogy, and geochemistry were analyzed by proximate analysis, inductively coupled plasma mass spectrometry, X-ray fluorescence spectroscopy, X-ray diffraction analysis, scanning electron microscopy-energy spectrum analysis, and incident light microscope. The enrichment regulations, distribution patterns, and occurrences of REY (rare earth element and yttrium) in coal under different geological conditions were compared. Geological significance and the influence of REY were then discussed. The average REY of Permian coal in the eastern margin of the basin is 127.9 μg/g, CC = 1.87, and the average REY of Carboniferous coal is 117.49 μg/g, CC = 1.72, which are within the normal enrichment range. The inorganic affinity of REYs in the study area is strong and mainly occurs in clay minerals and detrital phosphates and correlates well with LREY. The Permian coal sedimentary environment is more oxidized than the Taiyuan formation, and the Carboniferous coal sedimentary environment is noticeably more affected by marine water. With an increasing degree of coalification, the concentration of rare earth elements (REE) in high-rank coal vitrinite is lower than that in inertinite. In contrast, the concentration of REEs in low-rank coal is the opposite. This is because the oxygen-containing functional groups that can combine with REEs in vitrinite reduce significantly, resulting in the loss of trace elements into other forms. The provenance of the northern and central regions of the study area is mainly sedimentary rocks, granite, alkaline basalt, and continental tholeiite, while the southern region is mainly granite and sedimentary rocks.

1. INTRODUCTION

China is the world's largest coal and rare earth element (REE) producer. Both play important roles in the industrial economy and society. REEs are an important strategic resource in the high-tech field and are widely used in aerospace, modern electronic communications, and new energy fields. In the future, the industrial world's dependence on REEs will continue to increase. As a country with a large amount of rare earth resources, Figures 1 and 2 show that China controls more than 90% of the world's rare earth production.[1−3] According to the U.S. Geological Survey data,[4] China's REO (oxides of REY-lanthanides and yttrium) mine production accounted for more than 80% of global production between 2013 and 2017 but decreased to about 60% from 2018 to 2022 (Figure 1). However, China accounts for 35.2% of global REO mine reserves in 2023 (Figure 2), and the relationship between REO reserves and production is somewhat skewed. It is undeniable that China controls the vast majority of rare earth production. Although traditional resources are still relatively

Received: January 17, 2024
Revised: July 11, 2024
Accepted: July 11, 2024
Published: July 18, 2024

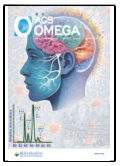

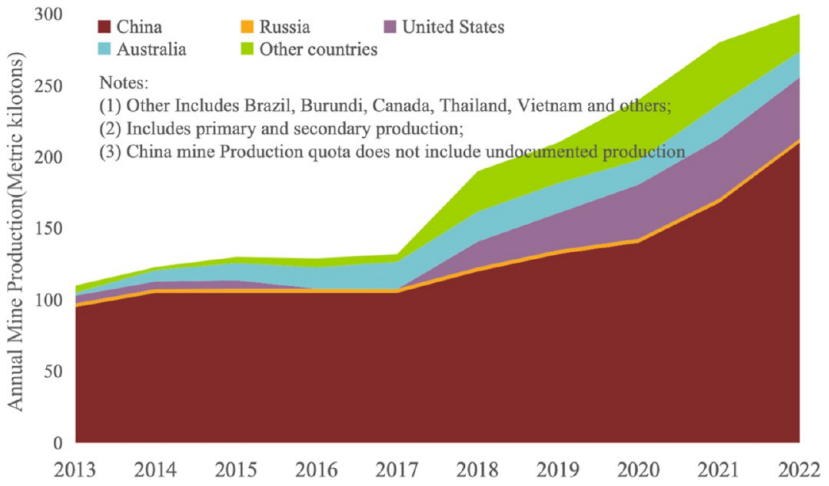

Figure 1. Global annual REO mine production (data from U.S. Geological Survey[4]).

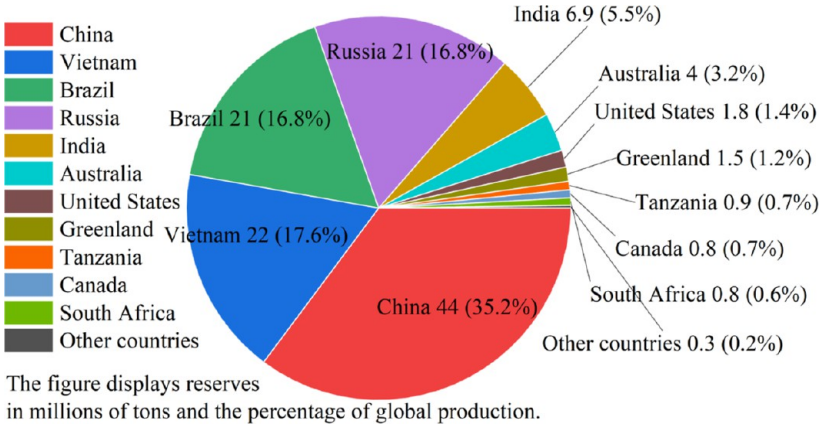

Figure 2. Global REO mine reserves (data from U.S. Geological Survey[4]).

plentiful, reserves are decreasing daily. Finding supplementary rare earth mineral resources would be of great strategic significance.

Coal ash contains many beneficial metal elements, such as germanium, gallium, lithium, uranium, and rare earths. Coal is used primarily as an energy source; predominantly for electricity generation, and is used, to a lesser extent, as a feedstock for chemicals and materials.[5,6] Advanced materials (such as coal-based products: carbon electrodes) and coal derivatives may offer attractive avenues for further research and development and could lay the groundwork for future manufacturing and processing,[7] particularly for REY (REE and yttrium) in coal and coal ash. The REY concentration in some coals and coal ashes is equal to or higher than that found within carbonatites, alkaline granites, and weathering crusts.[8−12] If extractable, this could be enormously economically beneficial. Additionally, the potential reduction of adverse environmental impacts due to the extraction of otherwise toxic metals from coal ash,[10,13−16] coal, and coal combustion byproducts (CCBs; e.g. fly ash, boiler slag) has been recognized as promising alternative sources for these critical elements.[17−21] Geochemical studies of coal mine drainage (CMD) show that mine drainage is often enriched in total REY.[22−25] Recently, there has been increasing research into coal, coal ash, and CMD for REY recovery.[6,10,12,14,26−28]

Many scholars[18,29−32] have proposed that the northern Ordos Basin in North China has ideal conditions for the development of large coal rare earth deposits. They suggest that REEs are enriched in coal in North China, controlled by both the material source and volcanic activity. Seredin and Dai[10] studied four genetic types (terrigenous, tuffaceous, infiltrational, and hydrothermal) of REY enrichment in coal basins. Montross et al.[20] found that REEs exist in coal ash as dispersed monomineralic grains, and they are fused with, or encapsulated within, amorphous aluminosilicate glass particles. This demonstrates that rare earth minerals from the coal are incorporated into aluminosilicate glass phases using traditional coal combustion processes. Lin et al.[33] used physical separation methods and step-by-step chemical extraction technology to maximize the extraction of REEs from coal ash. Additionally, Ziemkiewicz[34] and his team have developed a unique technique for recovering REE from what was initially thought to be low to moderately enriched postcoal mining waste.

Several studies have produced reliable experimental conclusions regarding the concentration of REY in coal. Finkelman[35] reported an average concentration of 62.1 μg/g in US coals. The world average for coal is 68.5 μg/g, while for coal ash, it is 404 μg/g. According to Dai et al.,[32] the estimated average amount of REY in Chinese coals is 137.9 μg/g, which is approximately twice the world average for coal. It is worth noting that slight variations in results may occur due to the use of different samples in the studies. Zhao and Tang (2002)[36] found that the average quantity of REE in Chinese coals was 72.003 μg/g. According to several studies,[10,13,37] a minimum

https://doi.org/10.1021/acsomega.4c00546
ACS Omega 2024, 9, 32481−32501

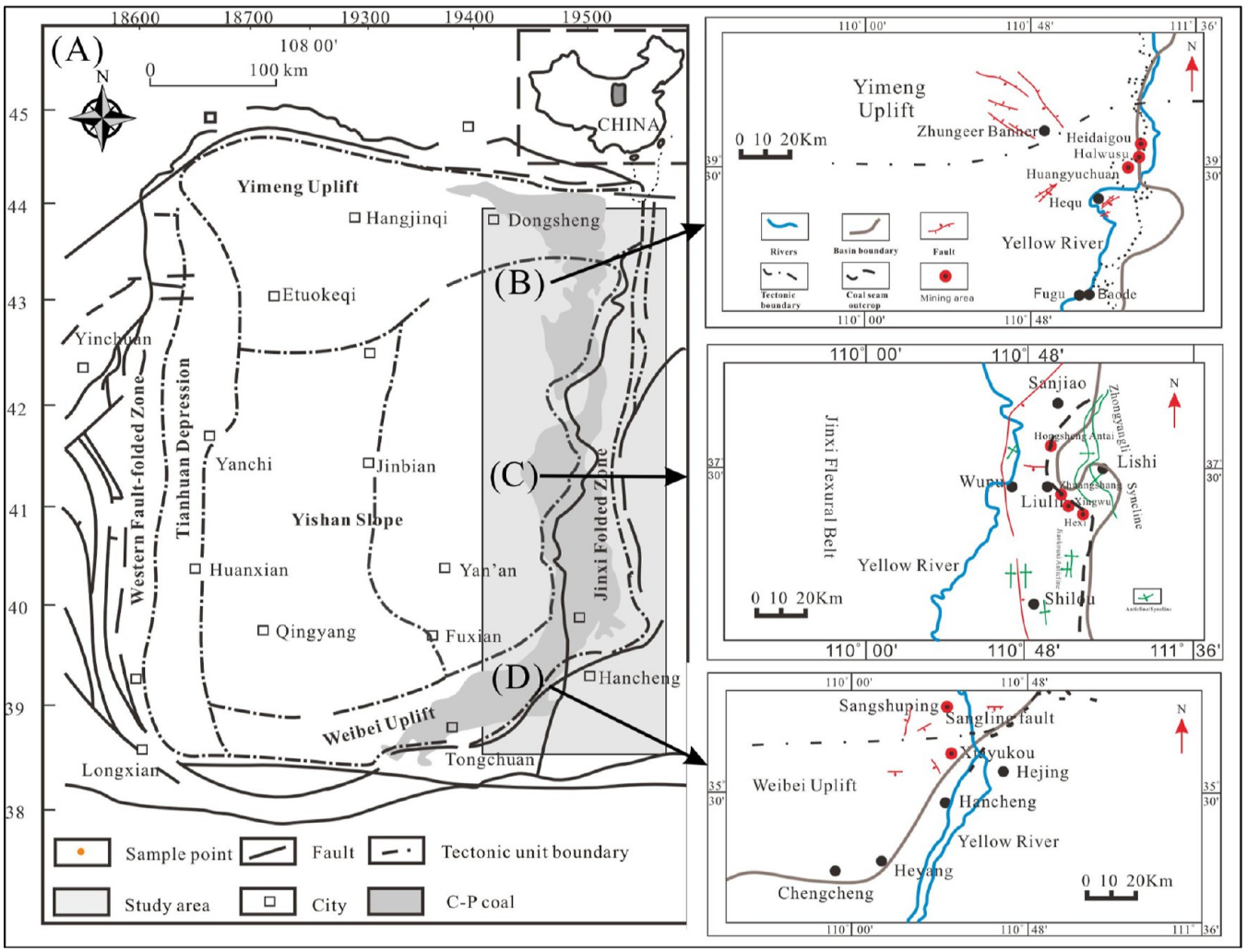

Figure 3. Tectonic units in the Ordos Basin (A); locations of the Jungar coalfield and sampling site (B); locations of the Hedong coalfield and sampling site(C); locations of the Weibei coalfield and sampling site (D).

REO concentration of 800−900 μg/g in coal ash is required for the beneficial retrieval of REE from coal. Zhang et al. (2015)[37] estimated the cutoff grade of REE in coal to be 115−130 μg/g on the coal basis and 677−762 μg/g on the ash basis. In recent years, there has been significant progress in innovative theoretical research on REEs in coal, particularly in the areas of abundance, material source, and mode of occurrence in the coal.

Seredin and Dai[10] created a convenient way of describing REY distribution in coals, by classifying the REY in coal into light (LREY—La, Ce, Pr, Nd, and Sm), medium (MREY—Eu, Gd, Tb, Dy, and Y), and heavy (HREY—Ho, Er, Tm, Yb, and Lu) groups. In order to show the variation characteristics of REEs in different coal samples, the study used a "three division method" to divide REEs, and Y was included with the REE. Normally, the average values of REY in chondrites, North American shales, or the upper continental crust (UCC)[38] are used to standardize the REY in research samples. This study aims to determine the average abundance and distribution of REEs in the majority of coal within the eastern margin of the Ordos Basin by selecting and analyzing samples from local coal mines. We also compare the enrichment factors, distribution patterns, and occurrence of REY in coal under different geological conditions and discuss the geological significance and influencing factor of REY.

2. GEOLOGICAL SETTING

The study area is located on the eastern edge of the Ordos Basin. The Jungar, Hedong, and Weibei coalfields were selected as research targets (Figure 3). The Jungar coalfield is located in the northeastern part of the Basin, spanning the northern slope of Shaanxi Province and the flexure fold belt of Western Shanxi Province. The internal structure is relatively simple, and only a few faults have developed. The coal-bearing rock series includes the Upper Carboniferous Benxi Taiyuan formations and the Lower Permian Shanxi formation,[39] The Taiyuan formation is a series of fluvial-delta-barrier coastal deposits. The thickness of the strata varies from 15 to 120 m, and the coal bearing capacity is high. There are 3−9 coal seams (Figure 4), of which no. 6 coal and no. 9 coal are the main coal seams with large thickness and stable development. The Shanxi formation is a set of terrigenous fluvial alluvial plain depositions. The thickness of strata varies from 40 to 110 m, with a gradual thickening trend from north to south, with 2−7 developed layers of coal (nos. 1−5 coal, Figure 4).

The Hedong coalfield is a large-scale coalfield from the late Paleozoic Carboniferous-Permian. It has an approximate

https://doi.org/10.1021/acsomega.4c00546
ACS Omega 2024, 9, 32481−32501

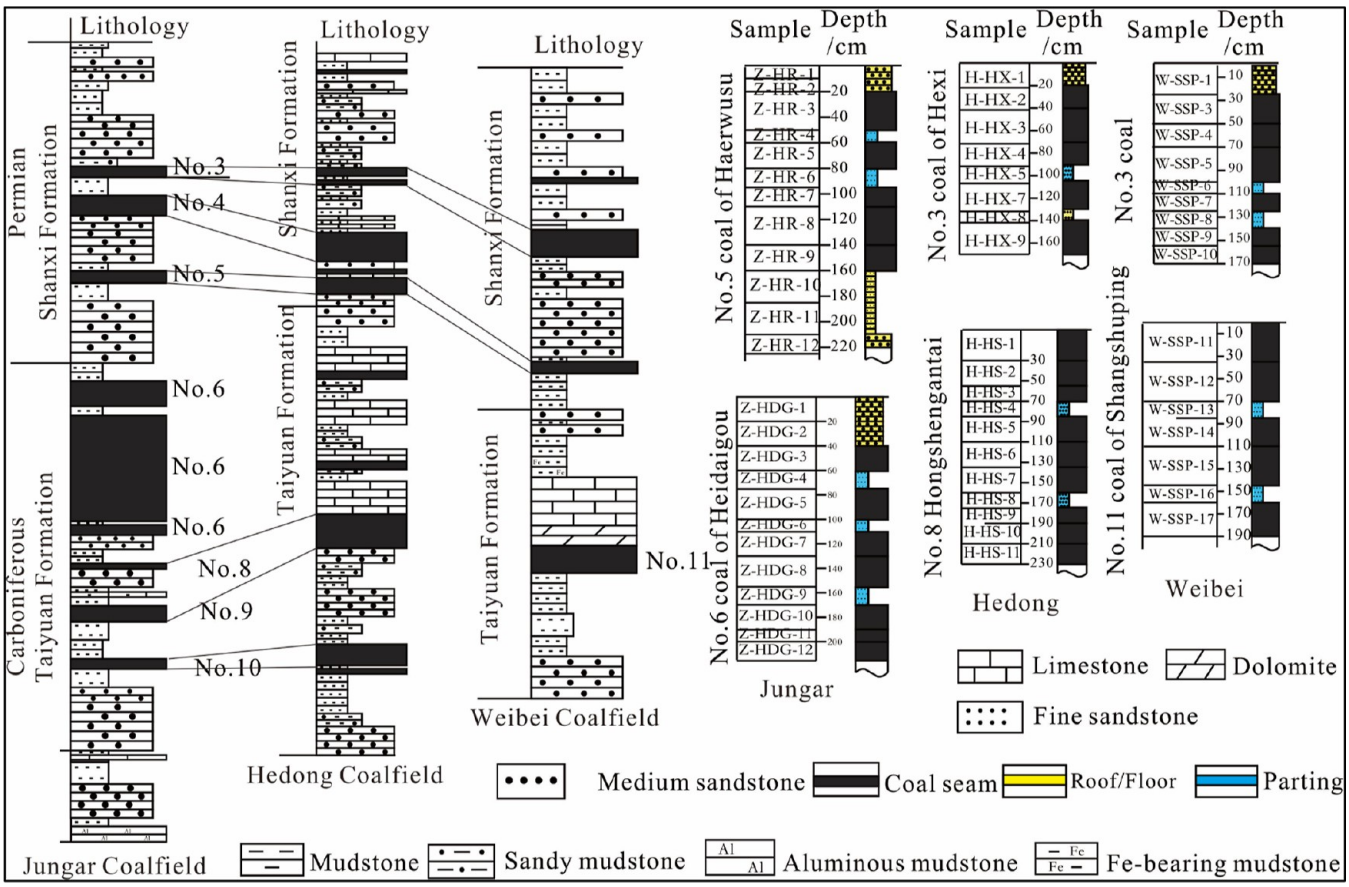

Figure 4. Distribution of Carboniferous-Permian sedimentary sequence, coal seams, and sampling positions in the eastern margin of the Ordos Basin.

north−south trend and a narrow strip distribution. The main coal-bearing strata include the Carboniferous Benxi formation, Taiyuan formation, and Permian Shanxi formation. The Taiyuan formation is a set of surface sea carbonate platform-barrier coast deposits. This group has a strata thickness that varies from 40 to 125 m, and it contains 3−7 coal seams of coal (nos. 6−10, Figure 4). The no. 8−9 coals are the exploitable coal seams with a thickness of more than 2 m, which were formed in the mudflat environment after regression, as reported by Zhao, Sun and Li.[40] Other coal seams may not have any industrial value or may be only locally recoverable. The Shanxi formation consists of fluvial-lacustrine-delta deposits, also described by Zhao et al.[40] The formation thickness varies from 25 to 90 m, with 2−7 developed layers of coal (nos. 1−5 coal). The main coal seams in this area are the no. 4 and no. 5 coals. The no. 3 coal can be locally mined.

The Weibei coalfield is situated southeast of the town of Ordos and within the eastern part of the Weibei uplift. It has a NE-SW zonal distribution, is approximately 190 km long from east to west, and is 25−50 km wide from north to south. The main coal-bearing rock series are the Carboniferous Taiyuan formation and the Permian Shanxi formation. The Taiyuan formation comprises clastic shore-delta sedimentary environments. The strata thickness ranges from 5 to 95 m, with 3−10 coal layers (no. 6 coal−no. 11 coal) developed. The no. 11 coal seam is the primary recoverable coal seam (Figure 4).

3. SAMPLES AND METHOD

3.1. Samples. This study selected eight mining areas from the Jungar, Hedong, and Weibei coalfields (Figure 3) and conducted channel sampling layer by layer from top to bottom, in accordance with ASTM Standard D2797/D2797M-11a (2011).[41] The 30 cm weathering layer on the channel surface was removed during sampling. The sample size was 10 × 10 × 10 cm (length × width × depth). A total of 59 samples were collected, consisting of 37 coal samples and 22 roof, floor, and parting samples. The samples included no. 6 coal from the Heidaigou mining area and no. 5 coal from the Haerwusu coalfield. Additionally, we collected samples from no. 8 coal in the Hongsheng−Antai coalfield, no. 3 coal from the Hexi and Sangshuping mining areas, and no. 11 coal from the Sangshuping coalfield (Table 1 and Figure 4). After the samples were collected, they were immediately placed in plastic bags to prevent contamination, oxidation, and water loss.

3.2. Methods. The following sample preparation procedures were used.

Low-temperature ashing (LTA) and X-ray diffraction analysis (XRD): The British EMITECH K1050X low-temperature plasma ashing instrument (power: 70 W, temperature: less than 180°) was used to conduct LTA to remove organic matter from the coal samples. The X'Pert PRO MPD automatic powder X-ray diffractometer produced by PANalytical in the Netherlands (voltage: 40 kV, current: 40 mA, X-ray target: Cu, measuring angle range: 5−70°, and angle measurement accuracy: ± 0.003°) was used to analyze the type and content of minerals following LTA.

https://doi.org/10.1021/acsomega.4c00546
ACS Omega 2024, 9, 32481−32501

Table 1. Sampling Information of Carboniferous-Permian Coal Seams in North China

coalfield	mine	coal	roof, floor, and parting	remarks
Jungar	Hedaigou	7	5	no. 6 Taiyuan formation coal
	Haerwusu	5	7	no. 5 Shanxi formation coal
Hedong	Hongsheng−Antai	9	2	no. 8 Taiyuan formation coal
	Hexi	5	3	no. 3 Shanxi formation coal
Weibei	Sangshuping	6	3	no. 3 Shanxi formation coal
	Sangshuping	5	2	no. 11 Taiyuan formation coal

Microscope observation; the mineralogy of the samples was examined using Leica DM4500 P and Nikon ECLIPSE LV100POL polarized light microscopy.

Scanning electron microscopy-energy spectrum analysis (SEM−EDX): After the coal samples were coated with gold, the S-4800 cold field emission scanning electron microscope, produced by Japan's HITACHI company, and the Czech TESCAN-VEGA\\LSH thermal field emission scanning electron microscope were used to observe the microscopic morphology and determine the constituent elements.

X-ray fluorescence spectroscopy: AxiosmAX X-ray fluorescence spectrometer produced by PANalytical in The Netherlands (voltage: 60 kV, current: 160 mA, power: 4.0 kW, SST-mAX type X-ray tube, accuracy: ± 0.0001°) was used to determine the major elements (SiO_2, Al_2O_3, Fe_2O_3, TiO_2, K_2O, Na_2O, CaO, MgO, P_2O_5) in coal from parting, roof, and floor.

Inductively coupled plasma mass spectrometry (ICP−MS): The ELEMENT XR plasma mass spectrometer produced by Thermo Science in Germany, was used to identify 44 elements; including trace elements and REEs + yttrium (REY) in coal from parting, roof, and floor. The specific steps are as follows: We weighed 0.05 g of the sample ground to 200 mesh (75 μm)

Table 2. Proximate Analysis and Total S and Micro—Component Content of Carboniferous and Permian Coals in the Eastern Margin of the Ordos Basin[a]

sample	Mad/%	Ad/%	Vdaf/%	St,d/%	vitrinite/%	inertinite/%	liptinite/%	mineral/%
Z-HDG-3	5.79	22.93	37.9	0.47	52.7	20.1	3.6	23.6
Z-HDG-5	5.63	19.92	35.6	0.31	45.6	29.3	2.2	22.9
Z-HDG-7	5.51	16.37	42.39	0.5	36.1	42.5	4.3	17.1
Z-HDG-8	6.19	29.31	24.2	1.21	39.2	37.6	9.2	14
Z-HDG-10	6.23	25.43	40.1	0.52	32.8	42.2	8.1	16.9
Z-HDG-11	5.91	21.8	39.3	0.67	30.3	36.9	7.8	25
Z-HDG-12	5.79	12.9	31.9	0.43	25.9	37.3	7.2	29.6
Z-HR-3	5.05	16.8	35.8	0.31	59.2	25.3	5.9	9.6
Z-HR-5	5.47	12.31	32.2	0.29	52.8	29.7	6.3	11.2
Z-HR-7	4.29	22.4	27.6	1.16	51.7	28.8	4.8	14.7
Z-HR-8	5.31	17.29	35.2	0.52	47.3	33.9	8.2	10.6
Z-HR-9	4.16	20.31	28.96	0.43	62.6	21.6	6	9.8
H-HS-1	0.95	25.12	16.15	3.97	52.1	25.9	12.7	9.3
H-HS-2	1.03	17.91	12.39	2.16	47.3	33.3	3.8	15.6
H-HS-3	0.72	15.75	25.41	3.05	66.2	27.2	0	6.6
H-HS-5	0.65	15.81	21.29	2.26	62.8	25.8	0.7	10.7
H-HS-6	0.99	17.38	18.26	4.32	58.8	23.6	10.2	7.4
H-HS-7	0.83	15.11	17.63	2.61	60.6	25.4	10.2	3.8
H-HS-9	1.31	22.92	15.97	1.73	61.2	16.8	8.8	13.2
H-HS-10	1.25	19.55	27.59	3.09	65.2	12.6	0	22.2
H-HS-11	2.21	16.03	29.05	1.97	77.2	13.9	1.4	7.5
H-HX-2	1.19	9.3	23.59	0.66	45.6	47.7	0.2	6.5
H-HX-3	1.35	11.18	19.22	0.62	51.1	39.5	0.4	9
H-HX-4	1.07	12.4	16.7	0.51	63.2	9.3	0	27.5
H-HX-7	1.56	18.02	22.08	0.41	65.2	30.2	0	4.6
H-HX-9	0.92	19.22	20.75	0.47	72	19.6	0	8.4
W-SSP-3	0.2	23.06	12.1	0.59	75.1	17.2	0	7.7
W-SSP-4	0.26	22.38	10.98	0.79	78.2	15.1	0.5	6.2
W-SSP-5	0.22	25.19	11.56	1.67	81.5	12.1	0.5	5.9
W-SSP-7	0.25	23.28	15.37	1.92	79.6	10.3	0	10.1
W-SSP-9	0.37	22.01	10.09	0.83	78.7	13.1	0.7	7.5
W-SSP-10	0.39	19.92	17.22	1.25	76.3	10.2	0.3	13.2
W-SSP-11	0.62	21.47	13.21	3.36	72.6	13.9	0	13.5
W-SSP-12	0.55	20.31	11.29	2.59	61.2	22.1	0.6	16.1
W-SSP-14	0.48	21.28	15.66	4.13	67.5	16.3	0.3	15.9
W-SSP-15	0.43	20.7	12.9	2.59	79.2	11.5	0.2	9.1
W-SSP-17	0.59	21.79	13.12	1.67	75.1	15.2	0	9.7

[a]M, moisture; A, ash; V, volatile matter; St, total sulfur of coal samples; ad, air-dry basis; d, dry basis; daf, dry and ash-free basis.

https://doi.org/10.1021/acsomega.4c00546
ACS Omega 2024, 9, 32481−32501

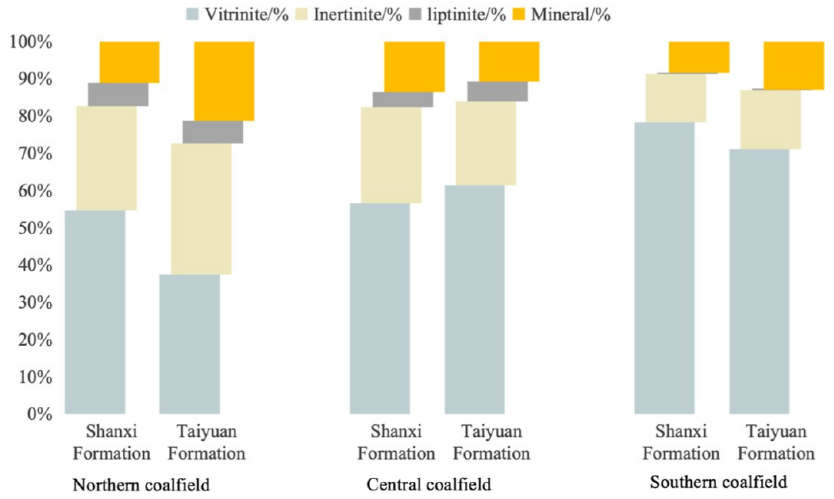

Figure 5. Distribution of the maceral content in Carboniferous-Permian coals.

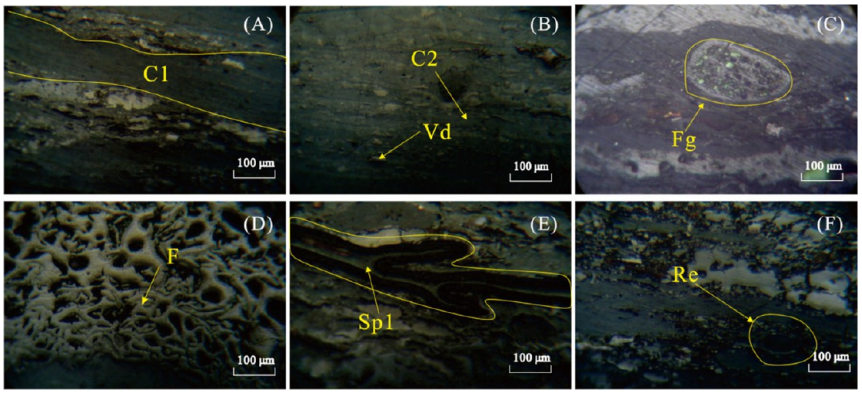

Figure 6. Microscopic characteristics of macerals in Carboniferous Permian coal in eastern Ordos Basin (500 times, immersion observation). (A) Heidaigou (Jungar coalfield), no. 6 Taiyuan formation coal, with strip collotelinite (C1); (B) Liulin area of Hedong coalfield, no. 3 Shanxi formation coal, collodetrinite (C2) and vitrodetrinite (Vd); (C) Haerwusu (Jungar coalfield), no. 5 Shanxi formation coal, funginite (Fg); (D) Liulin area of Hedong coalfield, no. 5 Shanxi formation coal, fusinite (F); (E) no. 6 Taiyuan formation coal Heidaigou (Jungar coalfield), megaspore (Sp1); (F) Hancheng (Weibei coalfield), no. 3 Shanxi formation, resinite (Re).

or less and placed it in a sample dissolving bottle filled with polytetrafluoroethylene. Next, we added 6 mL of analytically pure HNO_3, 0.5 mL $HClO_4$ (also analytically pure), and 2 mL HF (electronically pure). Seal and place on a 200 °C hot plate to heat for 48 h. After opening, evaporate the sample in the bottle until a gel is formed, add 2 mL of aqua regia, seal it, and place it on a 200 °C hot plate to heat for 24 h before digesting with HNO_3 (5%) to a sample solution, without precipitation. Finally, dilute to 50 mL for testing.

A heavy liquid centrifugal separation method is commonly used to separate macerals. The experimental process is as follows: grind coal samples of above 200 mesh in heavy liquid ($ZnCl_2$, 1.3 g/cm^3), heated evenly, and rest for 15 min to remove suspended solids and sediments. Then the residual liquid was uniformly poured into six centrifugal cups, and the rotation speed was controlled at 8000−10,000 rpm for 30 min. After centrifugation, the separated samples were put into an electrothermal dryer for drying (100°, 1 h) to separate the vitrinite from the inertinite. As only 2 g of sample was used for each separation, and the subsequent series of experiments generally required tens of grams of sample content, only Jungar no. 5 (low-rank coal) and Weibei no. 3 (high-rank coal) were separated in this experiment, and the proportions of vitrinite and inerinite after separation were in accordance with Table 2. Finally, the REE concentrations of the separated vitrinite and inertinite was tested by ICP−MS.

4. RESULTS

4.1. Macerals. The macerals found in Permian coal within the study area are mainly vitrinite. The macerals in the northern, central, and southern areas are 54.72, 56.54, and 78.23% vitrinite, respectively, and inertinite accounts for 27.86, 25.86, and 13.00%, respectively. The liptinite content within the whole area is low (<6%), and mineral content is about 10%. The percentages of vitrinite and inertinite in northern Carboniferous coals are similar; accounting for more than 70%, and the mineral content is also higher at 21.3%. The Carboniferous coals in the southern region are dominated by vitrinite (61.27, 71.12%), while inertinite accounts for 22.72 and 15.8%, respectively. The liptinite content is low (<6%), and the mineral content is about 10% (Table 2, Figure 5).

Among the coal macerals in the study area, collodetrinite and collotelinite are most common in the central and northern regions (Figure 6A,B). The vitrinite in the southern region is dominated by telinite and collodetrinite. Most cell structures are relatively intact, and the cell cavities are mainly filled with clay, calcite, pyrite, and other minerals. The whole region has the lowest corpocollinite content. It reflects the rapid

https://doi.org/10.1021/acsomega.4c00546
ACS Omega 2024, 9, 32481−32501

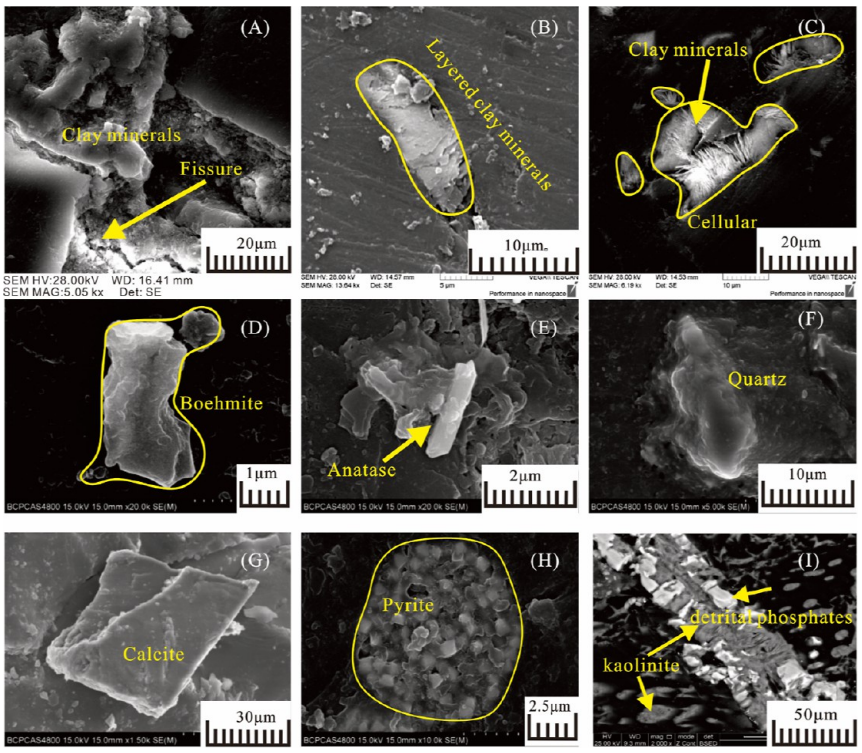

Figure 7. Microscopic characteristics of Carboniferous-Permian coal, eastern margin of the Ordos Basin. (A) no. 6 coal, filled in fractured clay minerals, 5050×, SEM (B) no. 5 coal, layered clay mineral, 13,640×, SEM (C) no. 3 coal, clay minerals filled in cellular, 6190×, SEM (D) no. 11 coal, boehmite, 20,000×, SEM−EDX. (E) no. 6 coal, anatase, 20,000×, SEM−EDX, (F) no. 3 coal, quartz, 5000×, SEM−EDX. (G) no. 5 coal, plate calcite, 1500×, SEM−EDX. (H) no. 11 coal, pyrite, 10,000×, SEM−EDX. (I) no. 3 coal, phosphate, 1420×, SEM−EDX.

sedimentary environment, indicating that the peatification process underwent strong gelatinization. Fusinite and semifusinite are the most common inertinites (Figure 6D). The cell structure of the fusinite is relatively clear; under oil immersion, it is white and yellow-white. The cell cavities are often filled with clay, calcite, pyrite, and other minerals, and occasionally funginite and inertodetrinite (Figure 6C). Microspores and megaspores are commonly found in the liptinite in the northern section of the study area (Figure 7E), microspores being the more numerous, and resinites are also occasionally present. The liptinite content in the southern area is low, and microspores are sometimes found. It was rare to find liptinites within the study area (<0.33%), with only a small amount of microspores and resinite found (Figure 6F).

4.2. Mineral Composition. Coal contains crystalline mineral particles, inorganic elements adsorbed or complexed by organic matter, and salts dissolved in pore water.[42] Most minerals in coal are detrital particles, either spherical, lenticular, band, or layer. Epigenetic minerals can fill fusinite and semifusinite cell cavities and internal cracks within the coal. Coal commonly contains mineral components such as aluminosilicates, carbonates, sulfides, phosphates, sulfates, chlorides, and other minerals, which include minerals that may be present in trace amounts or only detectable in trace amounts in various suites of coals.[43] Various methods, including optical microscopy, SEM−EDX, and LTA-XRD, have been used to observe and analyze the mineral composition of coal. The study area coal is primarily composed of aluminosilicate minerals such as kaolinite and Illite (Figure 7A−C), hydroxide minerals like boehmite (Figure 7D), carbonate minerals including calcite and high-mg calcite (Figure 7G), sulfide minerals such as pyrite (Figure 7H), oxide minerals such as quartz (Figure 7F) and anatase (Figure 7E), and detrital phosphates distributed on clay minerals in dense blocks (Figure 7I).

The mineral types and contents of the coal samples were determined by XRD after LTA. The results, shown in Table 3, indicate that the most abundant mineral in coal in the Ordos Basin study area is kaolinite, with the content ranging from 48.1 to 98.2% of total minerals, with a mean of 82.6%. Illite content varied from 10.2 to 45.2% with a mean of 25.4% of the total minerals. Boehmite was only found in two coalfields in the north and south source areas, and the content distribution range is 2.6 to 20.2%, and an average of 9.3% of total minerals. However, no boehmite was detected in the central region coal, which may be directly related to the absence of Al-bearing parent rock. Calcite content ranges from 1.2 to 7.6%, with an average of 3.1% of total minerals. The distribution range of pyrite was 0.3−5.3% of total minerals, with an average of 2.4%. The quartz content varies from 0.5 to 5.2% of total minerals, with an average of 2.0%. Siderite, anatase, and other mineral incidences are low, including sylvite, which is only visible in a few layers throughout the whole region.

4.3. REY Concentration in Coal. ICP−MS was used to analyze REEs and yttrium in Carboniferous-Permian coal from the eastern margin of the Ordos Basin. The concentration of the REEs and yttrium in coals was grouped into six categories using the CC index (Concentration Coefficient), as defined by Dai et al.[44] and presented in Table 4. CC > 100 (Unusually enriched), 10 < CC < 100 (significantly enriched), 5 < CC < 10 (Enriched), 2 < CC < 5 (slightly enriched), 0.5< CC < 2 (normal) and CC < 0.5 (depleted). In this study area, CC was mainly distributed in the range of 1.2−2.5, with an average value of 1.8, indicating normal enrichment. Relatively few areas

https://doi.org/10.1021/acsomega.4c00546
ACS Omega 2024, 9, 32481−32501

Table 3. Mineral Content of Carboniferous-Permian Coals in the Eastern Margin of Ordos Basin

sample	kaolinite/%	boehmite/%	illite/%	calcite/%	pyrite/%	siderite/%	quartz/%	anatase/%
Z-HDG-3	83	8.3		3.3	0.9		4.5	
Z-HDG-5	94.4	5.6						
Z-HDG-7	77.6	16.7		3.1	1.9	0.7		
Z-HDG-8	78.8	12.1		2.9	3.2		2.2	0.8
Z-HDG-10	93.1	6.9						
Z-HDG-11	74.9	20.2			1.3		3.6	
Z-HDG-12	77.8	17.3		1.8	0.8	1.1		1.2
Z-HR-3	85.3	10.1		1.2	0.9		2.5	
Z-HR-5	93			4.3			2.7	
Z-HR-7	94.1			3.2	2.7			
Z-HR-8	79.9		15.2		0.3	0.5	4.1	
Z-HR-9	79.5		18	2.5				
H-Z-1	93.1			3.6	0.8		1.9	0.6
H-X-1	95.7			3.2	1.1			
H-HS-1	89.6			4.4	3.5		1.6	0.9
H-HS-2	77.2		15.6	5.3	1.9			
H-HS-3	88.3			7.1	2.6	0.9	1.1	
H-HS-5	81.1		8.1	7.6	2.1	1.1		
H-HS-6	87.8			6.5	3.8	1.3	0.6	
H-HS-7	80.2		10.2	5.3	2.3	0.9		1.1
H-HS-9	94.7			3.1	1.5		0.7	
H-HS-10	78.6		12.3	5.9	3.2			
H-HS-11	93.1			4.2	2	0.7		
H-HX-2	93.7			2.8	1.3		1.5	0.7
H-HX-3	78		15.9	5.3	0.8			
H-HX-4	90.7			6.6	1.9			0.8
H-HX-7	75.8		20.1	3.2			0.9	
H-HX-9	98.2			1.8				
W-SSP-3	52		44.6	1.6	1.2		0.6	
W-SSP-4	96.2			1.9	0.6		1.3	
W-SSP-5	94.4			2.1	1.7	1.1	0.7	
W-SSP-7	54.1		39.8	2.4	1.5		2.2	
W-SSP-9	94.4			2.8	1.2		1.6	
W-SSP-10	52.8		42.7	3.6	0.9			
W-SSP-11	55		40.2	1.7	2.5	0.6		
W-SSP-12	95.4			1.3	2.8		0.5	
W-SSP-14	93.3			1.2	3.6		1.9	
W-SSP-15	48.1		45.2	2.7	3.2	0.8		
W-SSP-17	89.9			3.9	5.3		0.9	

showed lower enrichment in coal samples (no. 3 Shanxi formation coal in Sangshuping and no. 6 Taiyuan formation coal in Heidaigou).

Results show that the distribution of REY in no. 6 Taiyuan formation coal in the Jungar coalfield is 71.46 to 199.37 μg/g, with an average of 138.45 μg/g, which is higher than the average of REEs in world coal (68.42 μg/g) (Figure 8), CC = 2.1, The data shows that the enrichment level is more than double that of the world coal average but the same as the Chinese coal average. The distribution of REY in no. 5 Shanxi formation coal in the Jungar coalfield ranges from 8.30 to 131.47 μg/g, with an average of 77.52 μg/g. This is lower than the average of REY in Chinese coal (Figure 8), CC = 1.13, indicating normal enrichment. The distribution of REY in no. 8 Taiyuan formation coal in the Liulin area of the Hedong coalfield is 66.18−143.87 μg/g, with an average of 112.62 μg/g, CC = 1.6; no. 3 Shanxi formation coal is 71.33−161.24 μg/g, with an average of 116.53 μg/g, CC = 1.7. Both are lower than the REEs average in Chinese coal but higher than the world REEs average, indicating normal enrichment. REY in no. 11 Taiyuan formation coal in Hancheng (Weibei coalfield) ranges from 79.86−122.99 μg/g, with an average value of 101.41 μg/g, which is lower than the average value of REE in Chinese coal but higher than the average REE in world coal, CC = 1.48, indicating normal enrichment. The distribution of REY in no. 3 Shanxi formation coal is 121.56−165.73 μg/g, with an average of 148.20 μg/g, which is higher than the REEs average in Chinese coal, CC = 2.17, indicating slight enrichment.

Generally, from north to south in the eastern margin of the Ordos Basin, the concentration of REEs (REY) in Shanxi formation coal gradually increased and the REY in Taiyuan formation coal gradually decreased. The average REY of the Shanxi formation coal in the eastern margin of the basin is 127.9 μg/g, CC = 1.87, and the average REY of Taiyuan formation coal is 117.49 μg/g, CC = 1.72. There is little difference between them, and they show a lower than the Chinese coal REE average but higher than the REE world average.

https://doi.org/10.1021/acsomega.4c00546
ACS Omega 2024, 9, 32481−32501

Table 4. REE Concentration in Carboniferous-Permian Coal Seams of the Eastern Margin of the Ordos Basin (Whole Rock Base, $\mu g/g$)

Sample[a]		REY	La	Ce	Pr	Nd	Sm	Eu	Gd	Tb	Dy	Y	Ho	Er	Tm	Yb	Lu
China coal[b]		135.89	22.50	46.70	6.42	22.30	4.07	0.84	4.65	0.62	3.74	18.20	0.96	1.79	0.64	2.08	0.38
World coal[c]		68.42	11.00	23.00	3.40	12.00	2.00	0.43	2.70	0.32	2.10	8.40	0.57	1.00	0.30	1.00	0.20
roof	Z-HDG-1	173.21	45.90	40.60	10.50	39.60	6.46	1.02	5.20	0.68	3.09	16.40	0.59	1.45	0.23	1.29	0.21
roof	Z-HDG-2	381.52	88.10	163.00	16.90	61.30	9.69	1.37	6.29	1.01	5.11	21.30	0.99	2.56	0.45	2.94	0.51
coal	Z-HDG-3	139.51	15.80	35.60	4.62	19.70	4.68	0.77	5.04	0.94	6.68	34.70	1.40	3.84	0.69	4.35	0.71
parting	Z-HDG-4	23.92	0.82	2.98	0.56	3.05	1.04	0.22	1.46	0.16	1.53	9.79	0.25	0.86	0.14	0.86	0.20
coal	Z-HDG-5	149.86	25.50	47.16	6.12	22.76	5.63	0.59	5.09	0.61	2.53	27.73	0.72	1.98	0.22	2.97	0.25
parting	Z-HDG-6	13.99	3.60	5.69	0.52	1.70	0.18	0.04	0.22	0.05	0.25	1.31	0.06	0.13	0.02	0.19	0.04
coal	Z-HDG-7	80.49	18.50	33.20	3.40	11.10	1.61	0.30	1.56	0.25	1.38	7.12	0.23	0.75	0.16	0.82	0.11
coal	Z-HDG-8	199.37	29.50	62.00	6.97	26.80	6.32	1.27	6.33	1.32	7.54	42.40	1.27	3.48	0.54	3.21	0.42
parting	Z-HDG-9	38.26	3.12	6.05	0.68	2.71	1.00	0.28	1.64	0.36	2.99	14.80	0.57	1.41	0.36	2.02	0.27
coal	Z-HDG-10	175.46	31.22	59.13	6.56	25.31	6.21	0.71	5.37	0.67	1.98	30.95	0.63	2.01	0.68	3.82	0.21
coal	Z-HDG-11	71.46	8.22	16.00	1.91	8.05	2.16	0.41	2.51	0.55	3.97	20.60	0.83	2.69	0.37	2.81	0.39
coal	Z-HDG-12	152.99	44.20	67.80	5.96	16.60	2.04	0.36	2.04	0.36	1.81	8.95	0.36	0.93	0.18	1.20	0.20
parting	Z-HR-1	274.50	62.80	116.00	11.80	42.10	6.36	1.26	5.07	0.66	3.90	18.80	0.58	2.09	0.30	2.41	0.37
parting	Z-HR-2	277.37	54.60	109.00	11.80	42.80	6.94	0.91	6.26	0.93	5.66	31.00	1.00	2.67	0.44	2.93	0.43
coal	Z-HR-3	120.38	22.48	34.84	6.12	12.66	5.76	0.76	5.18	0.89	5.21	19.70	0.99	2.09	0.41	2.78	0.53
parting	Z-HR-4	129.47	13.80	28.80	3.81	14.70	4.56	0.96	5.01	1.30	7.37	38.90	1.34	3.77	0.54	3.98	0.64
coal	Z-HR-5	32.83	3.35	5.60	0.65	2.50	0.61	0.13	0.88	0.23	1.85	12.00	0.39	1.57	0.28	2.43	0.37
parting	Z-HR-6	225.66	38.90	73.20	7.59	27.00	5.92	1.21	6.36	1.27	8.05	46.00	1.52	3.72	0.68	3.70	0.54
coal	Z-HR-7	8.30	1.10	1.18	0.22	0.86	0.20	0.05	0.20	0.05	0.47	2.76	0.11	0.29	0.10	0.61	0.11
coal	Z-HR-8	94.62	27.50	18.05	2.89	7.38	1.76	0.25	1.74	0.35	3.06	24.30	0.92	2.93	0.51	2.58	0.40
coal	Z-HR-9	131.47	25.12	30.80	3.49	12.80	2.33	0.33	2.41	0.56	4.86	36.50	0.59	4.32	0.78	5.58	1.01
floor	Z-HR-10	314.18	75.10	119.00	12.90	43.00	6.91	0.84	5.82	0.93	6.30	34.40	1.06	3.41	0.51	3.45	0.55
floor	Z-HR-11	166.05	38.00	60.90	6.25	20.30	3.33	0.38	3.01	0.70	3.78	22.70	0.72	2.40	0.30	2.79	0.50
floor	Z-HR-12	473.74	105.00	178.00	22.70	78.20	12.60	1.15	10.70	1.55	9.22	42.20	1.27	4.68	0.79	4.92	0.76
coal	H-HS-1	66.18	13.86	16.47	2.74	9.81	1.63	0.15	1.84	0.27	1.47	15.46	0.34	0.89	0.31	0.75	0.20
coal	H-HS-2	137.48	29.51	49.43	5.88	17.83	4.12	0.62	3.23	0.55	3.17	19.66	0.61	1.11	0.22	1.37	0.17
coal	H-HS-3	119.47	25.21	38.51	4.32	15.76	3.51	0.58	2.92	0.42	2.69	21.62	0.56	1.39	0.26	1.43	0.29
parting	H-HS-4	5.13	0.79	1.39	0.16	0.55	0.11	0.03	0.20	0.02	0.18	1.35	0.02	0.12	0.00	0.18	0.02
coal	H-HS-5	93.19	16.76	27.52	4.27	16.02	2.76	0.47	2.12	0.48	2.25	17.17	0.41	1.36	0.16	1.26	0.18
coal	H-HS-6	123.50	24.65	36.77	6.52	20.97	3.25	0.61	2.91	0.56	2.63	20.68	0.45	1.62	0.18	1.49	0.21
coal	H-HS-7	143.87	28.66	40.43	6.96	25.93	4.02	0.71	3.52	0.61	3.05	25.19	0.61	2.03	0.21	1.70	0.24
parting	H-HS-8	42.21	10.90	13.40	1.59	5.76	0.98	0.29	0.79	0.14	0.87	6.24	0.16	0.52	0.07	0.43	0.08
coal	H-HS-9	121.24	22.89	35.13	5.57	21.57	4.32	0.75	2.79	0.58	2.29	20.43	0.46	1.95	0.26	1.97	0.28
coal	H-HS-10	114.71	25.68	39.17	4.92	17.82	3.15	0.61	2.16	0.49	1.95	15.11	0.31	1.78	0.17	1.28	0.11
coal	H-HS-11	93.95	16.80	31.60	3.51	12.50	2.47	0.44	2.44	0.55	2.80	17.20	0.47	1.43	0.25	1.24	0.24
roof	H-HX-1	283.26	53.30	107.00	11.80	45.10	8.01	1.48	7.61	1.11	6.11	32.60	1.09	3.19	0.49	3.85	0.51
coal	H-HX-2	71.33	12.91	15.86	1.72	9.82	1.70	0.93	1.91	0.44	3.27	17.79	0.51	1.59	0.42	2.02	0.45
coal	H-HX-3	108.77	19.32	32.19	5.13	16.71	3.18	0.69	2.21	0.59	3.05	22.79	0.39	1.13	0.23	0.97	0.19
coal	H-HX-4	81.25	17.90	28.10	4.69	11.30	2.52	0.38	1.95	0.39	2.16	9.71	0.28	0.82	0.15	0.79	0.11
parting	H-HX-5	239.62	49.60	89.00	9.89	35.50	5.74	0.85	5.47	0.88	5.57	28.40	1.06	3.32	0.54	3.24	0.56
coal	H-HX-7	161.24	35.31	63.22	4.52	21.23	3.54	0.79	2.43	0.49	3.16	22.68	0.59	1.27	0.21	1.61	0.19

https://doi.org/10.1021/acsomega.4c00546
ACS Omega 2024, 9, 32481−32501

Table 4. continued

Sample[a]		REY	La	Ce	Pr	Nd	Sm	Eu	Gd	Tb	Dy	Y	Ho	Er	Tm	Yb	Lu
parting	H-HX-8	239.91	51.23	92.12	7.66	37.68	6.58	0.73	2.99	0.57	3.87	31.18	0.52	1.93	0.27	2.26	0.32
coal	H-HX-9	160.06	31.20	57.68	6.72	29.13	5.19	0.59	2.51	0.51	2.97	20.61	0.36	1.11	0.12	1.21	0.15
roof	W-SSP-1	302.88	58.90	115.00	12.70	47.90	8.24	1.65	7.09	1.19	6.39	34.10	1.15	3.71	0.49	3.90	0.47
coal	W-SSP-3	127.16	29.30	52.10	5.77	20.70	3.07	0.51	2.21	0.25	1.71	9.26	0.30	0.87	0.14	0.85	0.12
coal	W-SSP-4	165.73	36.15	61.25	6.79	23.89	4.78	0.58	2.35	0.47	3.05	22.19	0.53	1.52	0.21	1.76	0.21
coal	W-SSP-5	152.75	31.78	59.17	6.05	18.47	3.67	0.61	1.68	0.38	2.76	25.13	0.47	1.06	0.16	1.19	0.17
parting	W-SSP-6	159.57	42.40	34.30	9.42	35.60	6.15	1.06	4.62	0.72	3.64	17.30	0.63	1.80	0.27	1.45	0.22
coal	W-SSP-7	151.24	33.23	58.92	7.19	23.76	3.93	0.55	2.29	0.53	2.58	15.29	0.59	0.85	0.22	1.12	0.19
parting	W-SSP-8	195.02	43.21	75.38	8.11	28.56	6.19	0.75	3.12	0.68	3.28	21.24	0.69	1.13	0.39	1.97	0.32
coal	W-SSP-9	170.79	39.65	65.29	7.47	27.18	4.36	0.59	2.87	0.41	1.93	17.05	0.76	0.97	0.52	1.39	0.35
coal	W-SSP-10	121.56	26.12	47.25	5.96	19.21	3.57	0.56	2.03	0.32	1.69	12.29	0.38	0.87	0.31	0.67	0.33
coal	W-SSP-11	79.86	19.10	24.10	2.27	7.91	1.74	0.37	2.04	0.51	2.69	15.30	0.54	1.45	0.24	1.33	0.27
coal	W-SSP-12	104.79	21.39	37.23	3.64	8.28	2.56	0.43	2.96	0.68	3.07	19.13	0.78	1.92	0.28	2.19	0.25
parting	W-SSP-13	236.14	49.96	92.23	9.66	32.19	5.02	1.12	5.32	1.02	6.05	25.66	1.02	3.16	0.39	2.98	0.36
coal	W-SSP-14	122.99	25.24	41.96	3.69	12.88	4.99	0.57	3.29	0.67	3.97	21.02	0.75	1.98	0.21	1.65	0.12
coal	W-SSP-15	89.77	20.05	31.28	2.41	7.71	2.93	0.49	2.42	0.52	2.87	15.08	0.49	1.57	0.15	1.63	0.17
parting	W-SSP-16	256.26	52.00	101.00	10.50	36.40	6.07	1.20	5.43	1.00	6.14	28.00	1.08	3.33	0.46	3.22	0.43
coal	W-SSP-17	109.62	21.76	39.68	4.34	7.19	2.03	0.56	3.15	0.65	4.17	21.76	0.64	1.53	0.32	1.39	0.45

[a]Whole rock base, μg/g. [b]Data from Taylor and Mclennan, 1985.[38] [c]Data from Ketris and Yudovich, 2009.[45]

https://doi.org/10.1021/acsomega.4c00546
ACS Omega 2024, 9, 32481−32501

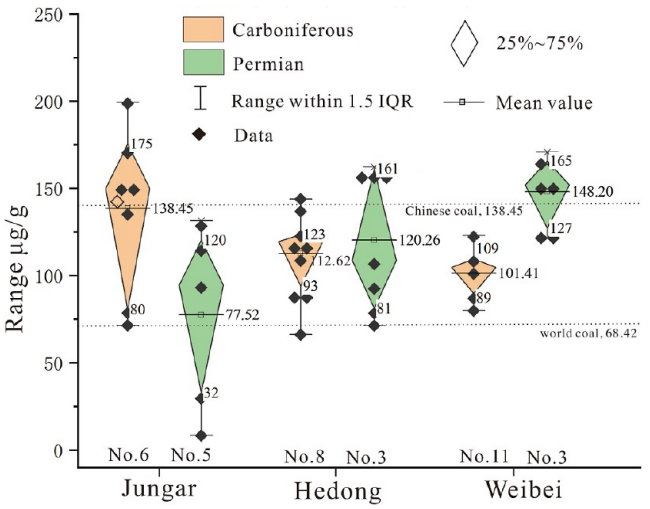

Figure 8. Comparison of REY concentrations of Carboniferous-Permian coals in the eastern Ordos Basin; interquartile range (IQR): the difference between the third quartile (Q3) and first quartile (Q1) is known as the IQR. (i.e.) IQR = Q3−Q1.

4.4. Geochemical Parameters of REY. *4.4.1. L/M, M/H, L/H.* The parameters L/M, M/H, and L/H represent the ratios of ∑LREY/∑MREY, ∑MREY/∑HREY, and ∑LREY/∑HREY, respectively. These ratios reflect the degree of differentiation among LREY, MREY, and HREY. A greater ratio value indicates an increased enrichment of certain REEs. Overall, the REEs in Carboniferous-Permian coals in the eastern margin of the Ordos Basin show the characteristics of ∑LREY > ∑MREY > ∑HREY, indicating that light REEs are more enriched than the medium and heavy REE. The L/M (3.5) and L/H (19.45) ratios of the Taiyuan formation coal are smaller than those of the Shanxi formation (3.78, 23.09), and the M/H (5.90) ratio is slightly greater than that of the Shanxi formation (5.74). The difference is not significant. From north to south, the L/M and L/H in Taiyuan formation coal gradually decreased, indicating that the differentiation between LREY and MREY, and the differentiation between LREY and HREY also gradually decreased. M/H in coal shows an increasing trend, indicating that the differentiation between medium rare earth and heavy rare earth is gradually increasing. The L/M, M/H, and L/H in the Shanxi formation coals, from north to south, gradually increased, indicating that the

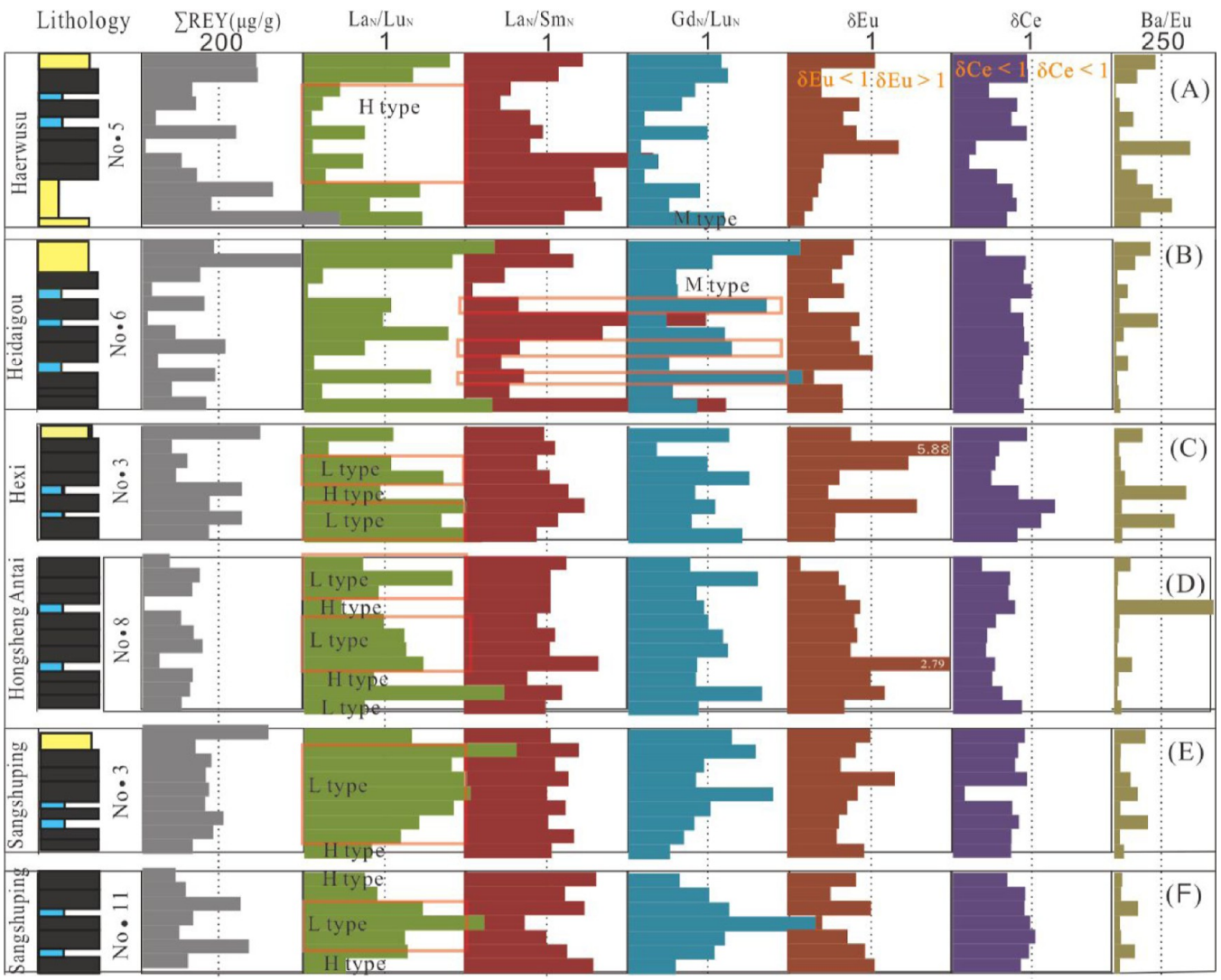

Figure 9. Vertical variations of ∑REE, $(La/Lu)_N$, $(La/Sm)_N$, $(Gd/Lu)_N$, δEu, and δCe about Carboniferous - Permian coals in the eastern margin of the Ordos Basin. (P)- Permian, (C)- Carboniferous. Standardized by UCC.

https://doi.org/10.1021/acsomega.4c00546
ACS Omega 2024, 9, 32481−32501

differentiation among light rare earths, medium rare earths, and heavy rare earths also gradually increased.

4.4.2. La_N/Lu_N, La_N/Sm_N, Gd_N/Lu_N. To compare the average concentrations of REY in coals with UCC data, as per La_N/Lu_N, La_N/Sm_N, and Gd_N/Lu_N, REE enrichment types can be split into three types: Light rare earth enrichment type (LREY): $La_N/Lu_N > 1$; Medium rare earth enrichment type (MREY): $La_N/Sm_N < 1$, and $Gd_N/Lu_N > 1$; and Heavy rare earth enrichment type (HREY): $La_N/Lu_N < 1$.[10,46] Figure 9 shows the REE types in the Carboniferous-Permian coal over the entire study area. Only a small part of the MREY enrichment type is present in Carboniferous no. 6 Taiyuan formation coals in Heidaigou (Figure 9B), or the M enrichment type appears in the column for the heavy enrichment type. There are two reasons for the M-enriched type: first, the MREEs are more easily adsorbed by humus adsorption than the LREEs, and second, the supply of acidic fluid in the basin.[47,48] Zhou et al.[49] and Dai et al.[9] point out that the M-enriched type is typical of acidic groundwater circulating in the basin. In some cases, acidic hydrothermal fluids can supply MREE to coal, such as in the Pavlovka coalfield[50] in the Russian Far East and the Songzao coalfield[51] in southwest China. The Harwusu no. 5 coal of the Shanxi formation is mostly the HREY enrichment type, with M-type occurring in the Floor (Figure 9A), and the Sangshuping no. 3 coal of the Shanxi formation is mostly the LREY enrichment type (Figure 9E). The remaining samples of Shanxi formation no. 3 (Figure 9C), Hongshen Antai Taiyuan formation no. 8 (Figure 9D) and Sangshuping Taiyuan formation no. 11 (Figure 9F) are of mixed enrichment types. This may be because the coal-forming swamps during the Carboniferous Taiyuan period were mainly located in coastal zones and were repeatedly flooded with marine water.[52] The REEs of coal in the Shanxi formation are mainly the LREY enrichment type. This is due to tectonic activity within the Permian Shanxi period and the large input of terrestrial materials.[53,54] The L-enriched type is typical of Chinese Palaeozoic high rank coals, where the REEs have a terrestrial source of detrital and volcanic ash genesis and were imported during the peat accumulation phase.[10] Dai and Finkelman[55] and Nechaev et al.[56] suggest that epigenetic acid leaching of many rare metals, including HREY, may lead to their redeposition and enrichment at the geochemical barrier of coal-bearing profiles. The geochemical barrier is represented by carbonate-rich coals and associated rocks, and the pH conditions of the depositional environments of the deposits are interpreted by using La/Y and La_N/Yb_N ratios as geochemical parameters. La/Y ratios >1 and <1 are associated with alkaline and acidic environments.[57,58] For the La/Y ratio in the no. 5 coal of the Jungar Mountain West formation, most of the samples are greater than 1, with an average value of 1.7, except for Z-HR-5 (La/Y = 0.28) and Z-HR-7 (La/Y = 0.40), which have very low REE concentrations. Thus, the no. 5 coal of the Jungar Shanxi formation forms a very localized alkaline environment favorable for HREY deposition.

4.4.3. δEu. δEu reflects the variation of Eu concentrations, which is useful in identifying provenance properties, reviewing diagenetic conditions, and in rock classification.[59] Sedimentary rock inherits REEs from its parent rock, and δEu can effectively identify likely constituent sources and is, therefore, a valuable tool.

$$\delta Eu = 2Eu_N/(Sm_N + Gd_N) \quad (1)$$

where Eu_N, Sm_N, Gd_N, are the values of Eu, Sm, Gd normalized to the UCC. Positive anomalies are represented by δEu > 1, negative anomalies by δEu < 1, and no anomalies by δEu ≈ 1. Several studies have demonstrated that Ba interferes with the assessment of Eu anomalies.[9,60,61] If Ba/Eu > 1000, the Eu value of the ICP−MS laboratory will be affected by BaO and BaOH, resulting in a higher Eu value.[9] The distribution of Ba/Eu in this study ranged from 10.68 to 603.33, with an average of 110.31, indicating credible results for Eu anomalies.

Most of the Carboniferous-Permian coals within the Ordos Basin eastern margin show Eu negative anomalies. The δEu of no. 6 coal of the Carboniferous Taiyuan formation in the Jungar coalfield varies from 0.27 to 0.89 with an average of 0.60, and the δEu of no. 5 coal of the Permian Shanxi formation in the Jungar coalfield varies from 0.43 to 1.38 with an average of 0.68. The δEu of no. 8 coal from Taiyuan formation in the Hedong coalfield varies from 0.17 to 1.21 (average 0.77), and that of no. 3 coal from Shanxi formation varies from 0.59 to 1.50 (average 1.08). The δEu of no. 2 and no. 3 Permian Shanxi formation coals in the Weibei coalfield varies from 0.61 to 1.33 (0.86 on average), and that of no. 11 Taiyuan formation coals varies from 0.44 to 1.08 (0.73 on average). The Eu in the Shanxi formation coal in the central and southern regions, and the Taiyuan formation has positive anomalies (Figure 9). δEu generally fluctuates only within its range of positive or negative anomalies. The phenomenon of alternating positive and negative anomalies is very rare. Research suggests that the provenance of the southern and central parts of the Ordos Basin have multiple Source area.[62,63]

4.4.4. δCe. δCe reflects the variation in Ce concentrations. Under a certain pH, in oxygen-rich sedimentary water, Ce^{3+} can be oxidized to Ce^{4+}, which separates from other REEs. If the water is oxygen-poor, Ce^{3+} maintains its original valence state.[64−66] Therefore, δCe is important in determining whether oxidation or reduction occurred within the sedimentary environment. Equally, Ce negative anomalies are important indicators of a marine sedimentary environment for sedimentary rocks.

$$\delta Ce = 2Ce_N/(La_N + Pr_N) \quad (2)$$

where Ce_N, La_N, and Pr_N are the values of Ce, La, and Pr normalized to the UCC. δCe > 1 represents positive anomalies, δCe < 1 negative anomalies, and δCe ≈ 1 no anomalies. The δCe < 1 of most samples in Carboniferous-Permian coals in the eastern margin of the Ordos Basin (Figure 9) mainly displays the characteristics of weak negative anomalies, suggesting that the overall sedimentary environment is somewhere between reduction and weak oxidation. Berry and Wilde[67] believed that water depth had an effect on the degree of redox in the formation water. Chen et al.[68] proposed that the typical δCe values are <0.5 in oxic marine water, ∼0.6−0.9 in suboxic marine water, and ∼0.9−1.0 in anoxic marine water. The water body in the Taiyuan formation coal seam is relatively deep in the central part of the eastern margin of the basin, and the sedimentary environment is significantly affected by marine water. The water bodies near the origin in the north and south are relatively shallow, and the sedimentary environment is weak oxidation. Much of the coal seam δCe in the Shanxi formation contains weak negative anomalies, indicating that the overall water depth during the coal-forming period was shallower than in the Taiyuan formation. Some coal seams have Ce negative anomalies, which may be associated with marine water intrusion.

https://doi.org/10.1021/acsomega.4c00546
ACS Omega 2024, 9, 32481−32501

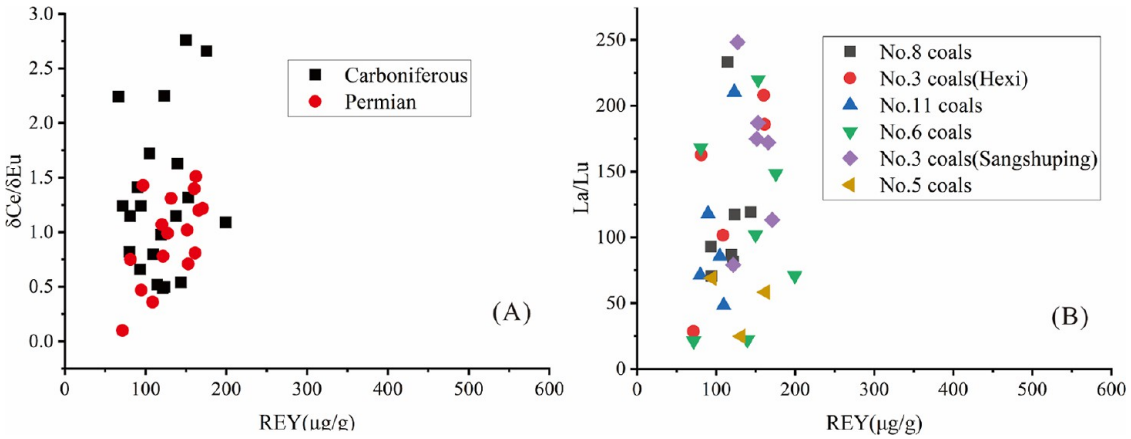

Figure 10. Relationship between δCe/δEu and ΣREY (A), relationship between La/Lu and ΣREY(B).

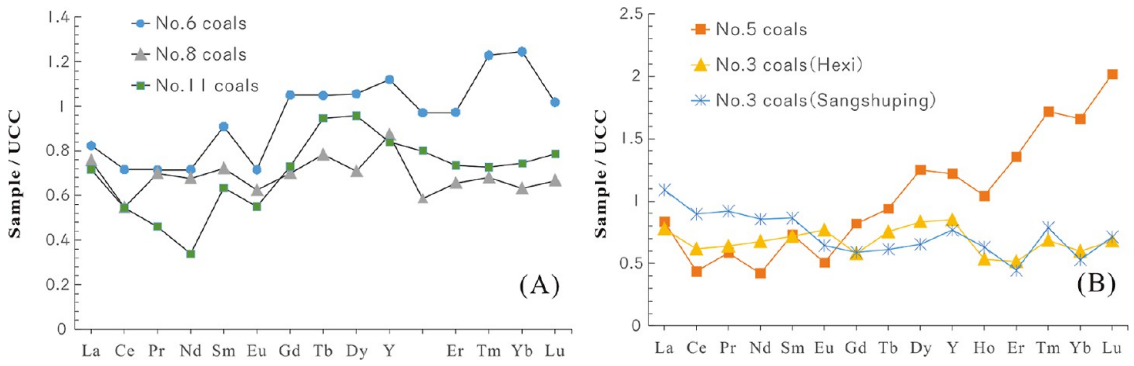

Figure 11. REY distribution patterns in coals of the eastern margin of the Ordos Basin. (A) Carboniferous (Taiyuan formation) coal in the North−southeastern margin of the basin. (B) Permian (Taiyuan formation) Coal in the North−southeastern margin of the basin.

Dai et al.[65] investigated the REY in Paleozoic coals in North China. The results indicated that a δCe/δEu value of less than 1 reflected an oxidizing environment, while a value greater than 1 indicated an acidic reducing environment during coal formation. In the diagram of δCe/δEu and ΣREE (Figure 10A), most of the Taiyuan formation coal samples have δCe/δEu values greater than 1, while those of the Shanxi formation are less than 1. The REE values of both coal groups are concentrated between 100 and 200 μg/g, indicating a relatively stable coal-forming environment affected by marine water and low supply of terrigenous debris. However, the environment of the Shanxi formation is more oxidized than that of the Taiyuan formation, which is consistent with previous discussions.[63,69] The La/Lu-ΣREY graph (Figure 10B) shows that the Taiyuan formation coals were affected by marine water, while HREY and LREY were retained in coal-forming swamps. Most of the coal in the Shanxi formation is relatively enriched with LREY, which concurs with the findings of Liu 1987[70] and Dai et al. 2003.[65] LREE is more enriched than HREE in continental freshwater environments. LREY and HREY in Shanxi formation no. 5 coal are enriched, which is believed to be related to the influence of groundwater leaching.

4.5. Distribution Patterns of REY in Coals. To reduce the influence of the "Oddo−Harkins" effect of REEs on the curve, the *x*-axis represents the number of protons of REE and the *y*-axis displays the normalized concentrations on a logarithmic scale (Figure 11). Distribution patterns of REEs in Carboniferous-Permian coals within the study area generally have uniform width, slight inclination, low differentiation of light rare earth, medium rare earth and heavy rare earth, and slight negative anomalies of δEu and δCe. This is also the common distribution pattern of REEs in marine-continental transitional facies coals.[71]

From north to south, the distribution pattern curves of REE in Taiyuan formation coal are mostly low on the left and high on the right (Figure 11), and Ce is typically slightly negative anomaly, reflecting that the coal-forming environment within the central region is the most reduced. Eu generally shows negative anomalies, and gradually changes to slightly negative anomalies toward the southern end. The differentiation of MREY is not obvious, and there is almost no difference between the north and south (Figure 11A). In the Shanxi formation coal REY distribution pattern curves, most of them are high on the left and low on the right, except for no. 5 coal (Figure 11B). Most of Ce shows weak negative anomalies, indicating that the overall sedimentary environment is dominated by weak reduction. Most of Eu has negative anomalies, with a gradual change from negative to positive southwards, which is related to the change in north−south provenance. The differentiation of MREY is not obvious, and there is minimal difference between north and south, which is consistent with the variation of the Taiyuan formation.

5. DISCUSSION

5.1. Mode of Occurrence of REE in Coal. The mode of occurrence of REEs in coals is complex, the types of modes of occurrence are defined by Dai et al. (2020),[72] who divided it into inorganic/mineral, intimate organic and organic associations. Inorganic/mineral combinations are defined as elements

https://doi.org/10.1021/acsomega.4c00546
ACS Omega 2024, 9, 32481−32501

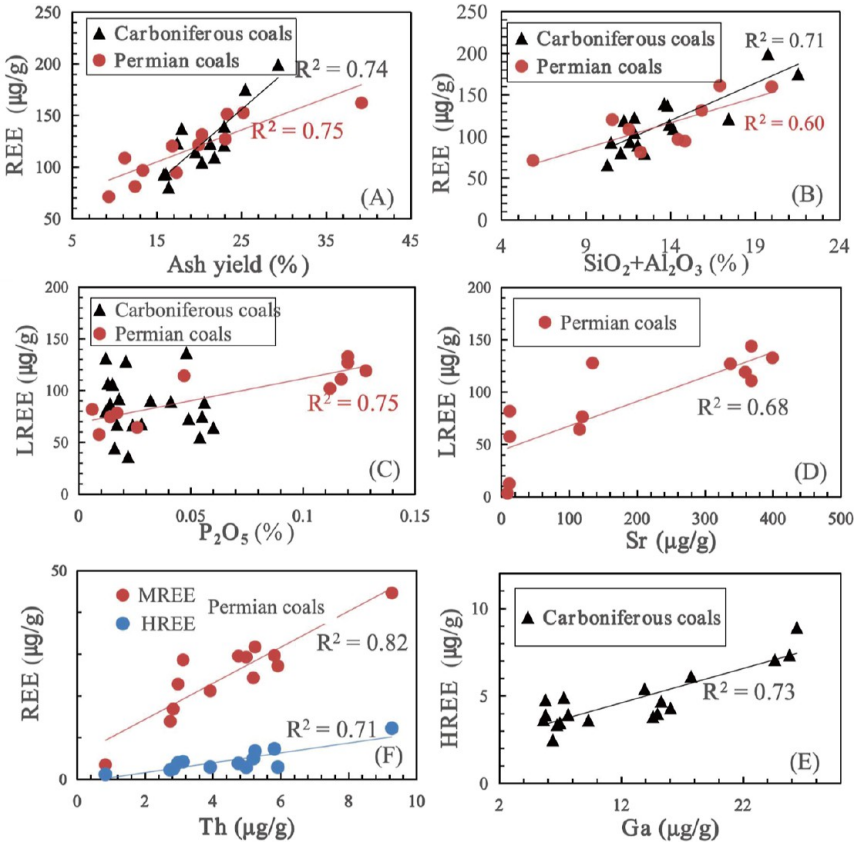

Figure 12. Relations of ash yield-REY(A), (SiO_2 + Al_2O_3)/%-REY(B), and (P_2O_5)/%-∑LREY(C); plot of Sr concentration versus LREE concentration (D); Th concentration versus MREE and HREE (E); and Ga concentration versus HREE concentration (F).

present in macroscopically and microscopically visible mineral or noncrystalline mineraloids. Finkelman et al. (2019)[73] have found more than 200 minerals in coal and its low-temperature ash. Minerals constitute the primary source of the majority of the elements in coal. Scholars[10,13,74,75] have discovered that REEs in coal are primarily found in clay minerals, aluminum phosphate, sulfates of the alunite supergroup, water-bearing phosphates, and carbonate. REEs can also occur on the surface or between layers of clay minerals and mica minerals in an ion-adsorbed state;[76−79] Intimate organic associations comprise micron-, submicron-, and nanoscale- minerals, elements adsorbed on the surface of organic matter, and elements dissolved in the pore water of coal or hosted in very fine-grained minerals.[72,80] Many studies have shown that different coal sources exhibit varying organic affinities for LREE and HREE.[32,81−83] The ionic radius determines that LREY is more likely to be enriched in Sr- and Ba-bearing minerals, while HREY is more likely to be enriched in Sc-, Hf-, and Zr-bearing minerals, which are extremely rare in coal; Organic association refers to the chemical bonding of organic matter, including carboxylates in low rank coal, with its constituent elements: carbon (C), hydrogen (H), oxygen (O), nitrogen (N), and sulfur (S). The present study investigates the mode of occurrence of REEs in Late Palaeozoic coals from the eastern margin of the Ordos Basin in minerals and macerals (including vitrinite and inertinite).

5.1.1. Minerals. Studies have shown a positive correlation between REYs concentrations in coal and ash yield.[10,36,65,84] This suggests that minerals play a crucial role in carrying REYs in coal. Many scholars[9,50,74,85,86] have found that REEs in coal are primarily present in phosphate minerals, which mostly originate as detrital minerals derived from the surrounding source rocks. Finkelman (1995)[85] and Dai et al. (2008)[32] demonstrated a positive correlation between REEs and ash yield, with clay minerals and phosphate minerals being the host minerals. This study found a positive correlation between REEs in Carboniferous-Permian coals and the coal ash yield (Figure 12A), with correlation indices of 0.74 and 0.75. This suggests that REEs in the coal of the study area may have an affinity with clay minerals and phosphate minerals.

The relationship between REY and the SiO_2+Al_2O_3 content shows that the two are positively correlated (Figure 12B). It implies that the REEs in coals associated with clay minerals or the detrital phosphates, chiefly due to weathering and denudation of parent rock. It was found in the study area that the detrital phosphate minerals in coal were mainly present in dense clumps within cell cavities or fractures, were often coincident with clay minerals (Figure 7I), and were mostly postgenetic. And by comparing the correlation analysis between REEs and P_2O_5 in Carboniferous-Permian coals, it was discovered that the concentration of LREY in Permian coal was positively correlated with P_2O_5 (R^2 = 0.75, Figure 12C). Additionally, Sr, Th, and LREE in coals showed significant positive correlations (R = 0.68 and 0.82, respectively; Figure 12D,F). This suggests that Permian REY also existed in detrital phosphate minerals. These findings are consistent with those of Wang and Dai et al. in the Late Permian 6 coals of the Harusu Coalfield in Inner Mongolia.[87] In Carboniferous coals, there is a strong positive correlation between Ga and HREE (R^2 = 0.73, Figure 12E). Additionally,

https://doi.org/10.1021/acsomega.4c00546
ACS Omega 2024, 9, 32481−32501

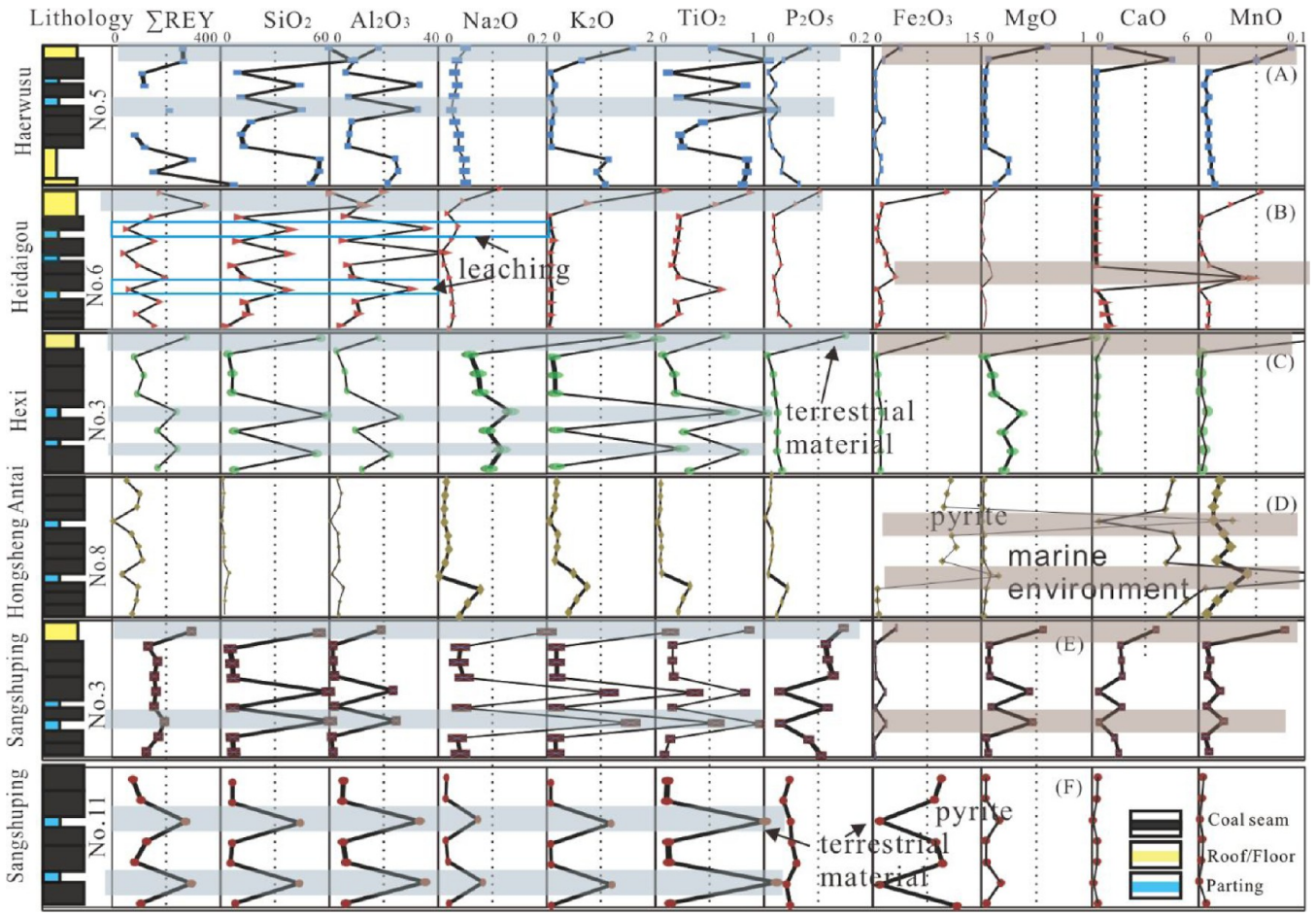

Figure 13. Vertical distribution of REY-major elements: (A) no. 5 coal seam of Shanxi formation in Haerwusu, (B) no. 6 coal seam of Taiyuan formation in Heidaigou, (C) no. 3 coal seam of Shanxi formation in Hexi, (D) no. 8 coal seam of Taiyuan formation in Hongshengantai area, (E) no. 3 coal seam of Shanxi formation in Sangshuping, and (F) no. 11 coal seam of Taiyuan formation in Sangshuping.

HREE shows a strong correlation with Li and Al_2O_3 (0.81 and 0.52, respectively). It is hypothesized that part of HREE in coals is related to Li due to the presence of the same carrier, clay minerals, or detrital phosphate minerals.

The Haerwusu no.5 (Figure 13A), Hexi coal mine no. 3 (Figure 13B), Sangshuping no. 3 (Figure 13E), and Sangshuping no. 11 coals (Figure 13F) demonstrate that REY in roofs, floors, and partings are higher than that in coals. Similarly, Al_2O_3, SiO_2, K_2O, Na_2O, TiO_2 and P_2O_5 show the same variable concentration, and most of these oxides are strongly affected by terrestrial material. It shows that the REE are derived from the detrital input and that they will correlate with ash yield. REY in roof rocks is higher (mean: 277.37 μg/g) and is lower in parting (mean: 25.39 μg/g). REY and major compounds Al_2O_3, SiO_2, K_2O, and Na_2O showed similar changes and correlated highly, and the REY concentration in parting is low. It is speculated that the low REE concentration in the parting is due to groundwater circulation, which brings REEs in parting into the underlying coal seam only in the form of leachate.[83,88] In addition, the sum of the percentages of these oxides, SiO_2, Al_2O_3, Fe_2O_3, MgO, CaO Na_2O, K_2O, MnO, TiO_2, and P_2O_5, shows that the percentages of roof and parting are 91.8 and 84.4, respectively, and the difference is not significant. It indicates that the content of Al_2O_3, SiO_2, K_2O, and Na_2O in roof and parting did not show deficiency. It is assumed that groundwater circulation only transports REY into parting in the underlying coal seam, by leaching.[8,89,90] Crowley, Stanton and Ryer[91] and Hower, Ruppert and Eble[64] studied the geochemical characteristics of REEs in coal containing volcanic ash and its alteration minerals in the United States. They found that the coal seam located in the lower part of the volcanic ash parting has REE concentrations several to tens of times higher than the overlying parting. The analysis shows that the enrichment of REEs in the coal seam is caused by groundwater leaching. In the no. 6 coal of the Jungar Coalfield located in the northern eastern edge of the Ordos Basin, the concentrations of REE in the partings are significantly lower than those in the underlying coal seams. This is believed to be due to leaching by groundwater.[32,92,93]

The concentration of REY in Hongsheng-Antai no.8 coal parting is low, and the concentrations of Al_2O_3, SiO_2, K_2O, Na_2O, TiO_2, and P_2O_5 are also found to be generally depleted. The concentrations of Na_2O, K_2O, TiO_2, and P_2O_5 were high in some samples (H-HS-9, H-HS-10, with ash yields of 22.92 and 19.55%, respectively), but still very low compared to other coal samples. This indicates that there is less terrigenous material compared to that of other coal samples. In addition, the amount of Fe_2O3, MgO, CaO, and MnO in partings is significantly higher than coal samples (Figure 13D). The formation of parting is caused by marine water flow, and the REY in marine environments is not enriched.[54,66,94] This is another reason for the low REY concentration in parting.

https://doi.org/10.1021/acsomega.4c00546
ACS Omega 2024, 9, 32481−32501

The REY in the roof and parting of the Sangshuping no. 3 coal seam is higher than coal, and the REY shows the same variation with major oxides Al_2O_3, SiO_2, K_2O, Na_2O, and TiO_2. However, correlation between REY in the coal and these major compounds is not clear. The contents of MgO, CaO, and MnO are also high (Figure 13E). It is believed that REEs are not only a terrestrial material, but the concentration of REY may also have been affected by other factors, such as marine water. Seawater is enriched in both LREE and HREE. Additionally, REE distribution in seawater exhibits a significant deficiency of Ce. The deficiency of Ce may be due to oxidation of Ce^{3+} to Ce^{4+} and precipitation from solution as CeO_2 under marine conditions, while other REEs still retain the valence state of +3.[95−97] Figure 9A,D,E demonstrate that the no. 5 coal of Shanxi formation in Haerwusu Coalfield, the no. 8 coal of Taiyuan formation in Hongshen Antai Coalfield and the no. 3 coal of Shanxi formation in Sangshuping Coalfield exhibit obvious Ce-negative anomalies, suggesting that these samples were affected by seawater during the coal formation process. REY in no. 11 coal seam partings is higher than that in coal. REY in coal and parting is positively correlated with major compounds Al_2O_3, SiO_2, K_2O, Na_2O, TiO_2, and P_2O_5, and negatively correlated with Fe_2O_3, CaO, and MnO. It shows that the formation of parting and the source of REYs are mainly initiated by terrigenous matter. The partings in the no. 11 coal seam are primarily composed of claystone and can be divided into two sections. The upper section is unevenly distributed and has a thickness of approximately 0.1 m, while the lower section is a kaolinite layer with a consistent thickness of 0.2 m.[54] This is consistent with the characteristics of "tonstein" volcanic sediments, which is a type of parting in coal formed by volcanic ash.[51,91] In addition. The no. 11 coal seam is situated in the lower section of the Taiyuan formation and was deposited in a delta sedimentary system.[54] The negative Ce anomaly is not obvious or slightly positive, indicating that there is less seawater influence and no leaching, so the REE concentrations in the partings of Sangshuping mining area (sample W-SSP-13, W-SSP-13, mean value: 246.2 μg/g) are significantly higher than that in the coal (mean value: 101.4 μg/g).

5.1.2. Macerals. With the aid of a high-speed centrifuge, the macerals with a density greater than that of the heavy liquid ($ZnCl_2$, 1.3 g/cm^3) sink under centrifugal force to obtain the inertinite, which consists mainly of fusinite, semifusinite, funginite, and secretinite; the macerals with a density less than that of the heavy liquid float up to obtain the vitrinite, which consists mainly of telinite, collodetrinite, and collotelinite. As only 2 g of sample was used for each separation, and the subsequent series of experiments generally required tens of grams of sample content, only Jungar no. 5 (low-rank coal) and Weibei no. 3 (high-rank coal) were separated in this experiment, and the proportions of vitrinite and inerinite after separation were in accordance with Table 2. Finally, the REE concentrations of the separated vitrinite and inertinite was tested by ICP−MS (Table 5).

In addition to minerals in coal, organic matter can also be enriched in REEs. This study shows that the REY in the vitrinite of low-rank coal is greater than that in inertinite (Table 5, Figure 14), and the opposite phenomenon occurs in high-rank coal. Senesi and Adriano[98] divided trace element and organic matter binding states into two complex types; covalently bonded internal complex compounds of metal ions and organic molecules, and electrostatically attracted

Table 5. REE Characteristics of Vitrinite and Inertinite in Carboniferous-Permian Coal in the Eastern Ordos Basin

sample	Z-HR-O3 (low-rank coal)	Z-HR-O2 (low-rank coal)	W-SSP-O1 (high-rank coal)	W-SSP-O1 (high-rank coal)
macerals	vitrinite	inertinite	vitrinite	inertinite
REY	63.31	47.55	80.66	93.52
LREY	45.15	28.46	55.64	64.72
MREY	14.63	14.67	20.74	24.92
HREY	3.24	4.3	3.92	3.46
$(La/Lu)_N$	0.77	0.3	0.8	0.74
$(La/Sm)_N$	1.46	1.44	1.76	1.21
$(Gd/Lu)_N$	0.75	0.23	0.67	0.8
ΔEu	0.8	0.78	0.89	0.85
ΔCe	0.75	0.83	0.8	0.94
La	15.39	9.35	20.1	17.6
Ce	17.13	13.7	23.67	29.7
Pr	1.75	1.51	2.27	2.92
Nd	9.3	5.29	7.89	12.31
Sm	1.58	0.903	1.71	2.19
Eu	0.3	0.191	0.36	0.41
Gd	1.89	0.89	2.12	2.39
Tb	0.27	0.23	0.5	0.45
Dy	1.41	1.79	2.67	2.58
Y	11.06	11.76	15.45	19.5
Ho	0.24	0.36	0.55	0.55
Er	0.8	1.53	1.22	1.31
Tm	0.17	0.27	0.25	0.29
Yb	1.82	1.82	1.63	1.06
Lu	0.21	0.33	0.27	0.25

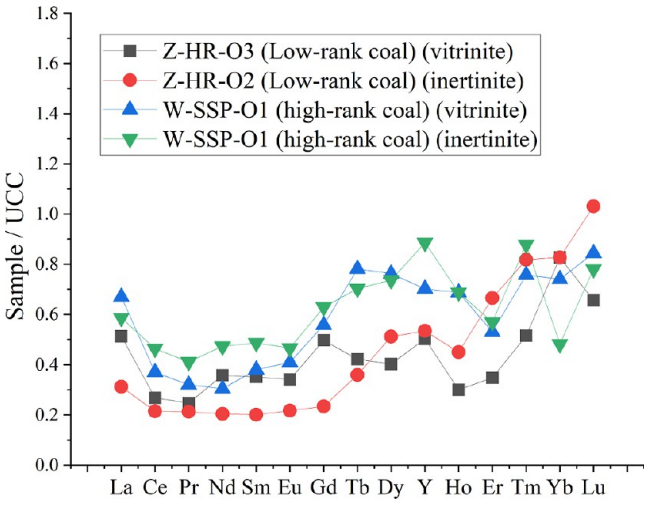

Figure 14. REY Distribution patterns of macerals in Carboniferous-Permian coal, eastern margin of the Ordos Basin.

unstable, easily dissociated external complexes. In coals with low coalification, trace elements ionically bound to hydroxyl (−OH), carboxyl (−COOH), sulfhydryl (-SH) and amino (−NH) groups.[99] It is surmised that during the early coalification process, REY and organic matter combined simultaneously with the two complexes. In high-rank coals, an increase of the coalification degree and temperature causes the aromatic structure of vitrinite to chemically change, losing large numbers of oxygen-containing functional groups. As a result, the REYs that are bound by electrostatic attraction are then lost but REYs in the form of internal complexes are

https://doi.org/10.1021/acsomega.4c00546
ACS Omega 2024, 9, 32481−32501

preserved. The internal complex is inherited mainly from low rank coal,[72] but the inertinites are relatively stable during this process. Therefore, the REY in high-rank coal vitrinite is lower than that in inertinite, which is the opposite to low-rank coal.

There are three possible causes of enrichment of REEs, by organic matter, in coal: ①REEs can be absorbed by coal-forming plants and accumulate and enrich, but the enrichment mode is very limited, and the concentration of absorbed REEs is very small. ②Peat swamp is an acidic environment, and each part of the plant has a strong adsorption capacity in the gelation process, which can adsorb some REEs dissociated from clastic minerals. ③When the coal seam is formed, the REEs in the overlying rock can be adsorbed by coal organic matter under acidic conditions through leaching.

The $(La/Lu)_N < 1$ of vitrinite and inertinite, and the REY distribution pattern curves of organic macerals in coal (Figure 14) are mostly low on the left and high on the right, indicating that HREY is the enrichment type, and that low rank coal is easier to enrich. HREY, δEu, and δCe are negative anomalies, and the δCe of inertinite is greater than that of vitrinite. It also shows that the water depth of the inertinite formation is shallow and the oxidation condition is stronger than vitrinite.

5.2. Provenance Analysis. The Ordos Basin during the Late Paleozoic had a paleogeographic pattern of north−south uplift and central depression. The Carboniferous-Permian terrigenous material in the northern Ordos Basin mainly comes from Yinshan ancient land on the northern side, while the terrigenous material in the southern Ordos Basin comes from the North Qinling orogenic belt.[100]

The chondrite average value[38] was used for standardization to show the provenance characteristics of parent rocks. Comparison of REE distribution patterns in coal after standardization is shown in Figure 15. The Permian and

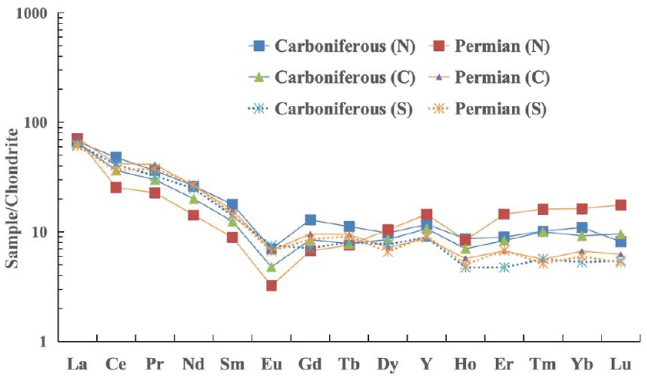

Figure 15. Chondrite-normalized plot-REEs in Carboniferous-Permian coals of the Ordos Basin.

Carboniferous coal seams in the northern, central, and southern parts are consistent. Comparison shows that the LREY segment strike is basically the same, and the difference between the MREY and HREY segments becomes more evident. The Eu anomalies in the northern and central coals are clearly negative, while Eu anomalies in the southern coals are slightly negative anomalies and positive anomalies. There were also significant differences at Tm and Yb, indicating that the distribution patterns of REEs in different sources after standardization are inconsistent.

Allègre and Minster[101] proposed the use of $\omega(La)/\omega(Yb) - \omega(\sum REE)$ diagrams to identify rock genesis, before analyzing the source of sediments and parent rock properties origin. We used the same method to identify the origin, nature, and change of features within the study area (Figure 16). Most of

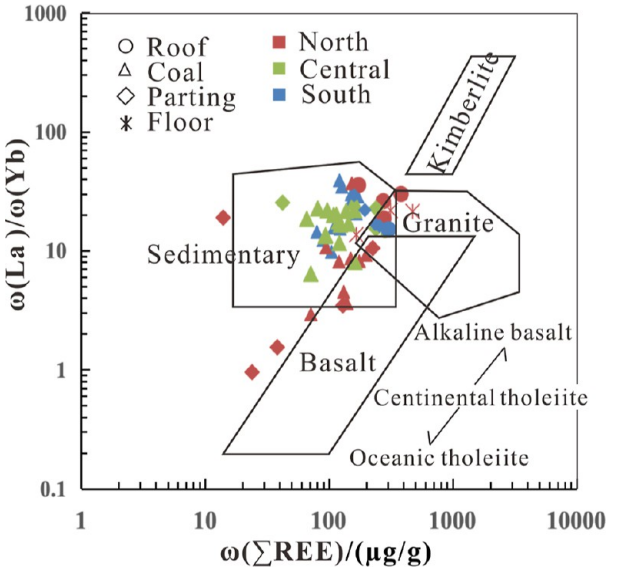

Figure 16. Crossplot of $\omega(La)/\omega(Yb) - \omega(\sum REE)$ of Carboniferous-Permian coals.

the coal samples are located in the sedimentary rock area of the crossplot, and most of the roof and floor samples are located in the sedimentary rock, granite, alkaline basalt and continental tholeiite areas of the crossplot. The parting samples are scattered in the crossplot, and some are outside the diagram lithology (Figure 16), possibly due to groundwater leaching, which would remove REY. The diagram supports that the similarity of provenance in each mining area is very high, and they mainly have the combined characteristics of mixed lithology.

6. CONCLUSIONS

(1) The average REY in the Permian coal in the eastern margin of the basin is 127.9 μg/g, CC = 1.87, and the average in Carboniferous coal is 117.49 μg/g, CC = 1.72, which fall within the normal enrichment range. The mineability of rare earth ore is fairly low and is lower than the $\sum$REE average in Chinese coal, but higher than the $\sum$REE average in world coal. M-REY enrichment only appears in Heidaigou Carboniferous no. 6 coals, Haerwusu Permian no. 5 coals show H-REY enrichment, and Sangshuping Permian no. 3 coal is of the L-REY enrichment type, and the rest are mixed enrichment.

(2) REYs in coals in the study area have a strong inorganic affinity and mainly occur in clay minerals and detrital phosphates. The ability of pyrite and calcite to enrich REYs is low. In addition to inorganic minerals in coal, organic matter can also be enriched in REYs. Results show that the REY in low-rank coal vitrinite is greater than in inertinite, with the opposite phenomenon occurring in high-rank coal. This is because as the coalification degree increases, the increase in temperature triggers the disappearance of oxygen-containing functional groups that can combine with REYs in

https://doi.org/10.1021/acsomega.4c00546
ACS Omega 2024, 9, 32481−32501

vitrinite. This leads to the loss of REYs. The $(La/Lu)_N$ < 1 of vitrinite and inertinite indicates that the REYs in organic matter are mainly of the H-REY enrichment type. δEu and δCe show negative anomalies, and most of the δCe in inertinite is larger than in vitrinite.

(3) distance from the source mainly determines the coal REY concentration in the study area, and a change of source will affect the normalized distribution pattern. In general, marine water intrusion affects the REYs distribution pattern, making the negative anomaly at Ce significantly larger, while the leaching of acidic formation water may increase coal REYs concentration. The provenance in the northern and central regions of the study area is mainly from sedimentary rocks, granite, alkaline basalt, and continental tholeiite areas, while the southern region provenance is mainly from granite and sedimentary rock areas.

AUTHOR INFORMATION

Corresponding Authors

Wenhui Huang − *School of Energy Resources, China University of Geosciences, Beijing 100083, China; Key Laboratory for Marine Reservoir Evolution and Hydrocarbon Abundance Mechanism, School of Energy Resources, China University of Geosciences, Ministry of Education, Beijing 100083, China;* orcid.org/0000-0002-9623-2652; Email: huangwh@cugb.edu.cn

Yuanfu Zhang − *School of Energy Resources, China University of Geosciences, Beijing 100083, China; Institute of Earth Sciences, China University of Geosciences, Beijing 100083, China;* orcid.org/0000-0003-3116-3446; Email: zhangyuanfu@vip.163.com

Authors

Long Wen − *School of Energy Resources, China University of Geosciences, Beijing 100083, China; Key Laboratory for Marine Reservoir Evolution and Hydrocarbon Abundance Mechanism, School of Energy Resources, China University of Geosciences, Ministry of Education, Beijing 100083, China; Institute of Earth Sciences, China University of Geosciences, Beijing 100083, China;* orcid.org/0000-0002-5604-5297

Bo Jiu − *School of Energy Resources, China University of Geosciences, Beijing 100083, China; Key Laboratory for Marine Reservoir Evolution and Hydrocarbon Abundance Mechanism, School of Energy Resources, China University of Geosciences, Ministry of Education, Beijing 100083, China*

Deyu Yan − *School of Energy Resources, China University of Geosciences, Beijing 100083, China; Key Laboratory for Marine Reservoir Evolution and Hydrocarbon Abundance Mechanism, School of Energy Resources, China University of Geosciences, Ministry of Education, Beijing 100083, China*

Ruilin Hao − *School of Energy Resources, China University of Geosciences, Beijing 100083, China; Key Laboratory for Marine Reservoir Evolution and Hydrocarbon Abundance Mechanism, School of Energy Resources, China University of Geosciences, Ministry of Education, Beijing 100083, China*

Huidi Hao − *School of Energy Resources, China University of Geosciences, Beijing 100083, China; Key Laboratory for Marine Reservoir Evolution and Hydrocarbon Abundance Mechanism, School of Energy Resources, China University of Geosciences, Ministry of Education, Beijing 100083, China*

Complete contact information is available at: https://pubs.acs.org/10.1021/acsomega.4c00546

Author Contributions

Long Wen: Conceptualization, Sampling, Methodology, Writing-Original draft preparation. Yuanfu Zhang and Wenhui Huang: Funding acquisition, Supervision. Yuanfu Zhang: Writing—Review and Editing. Bo Jiu, Sampling, Investigation. Deyu Yan: Investigation. Ruilin Hao: Sampling, Data curation. Huidi Hao: Investigation.

Notes

The authors declare no competing financial interest.

ACKNOWLEDGMENTS

This work was financially supported by the Natural Science Foundation of China (grant nos. 42272201), the National key research and development program (grant no. 2021YFC2902003), and the National Science and Technology Major Project (grant no. 2017ZX05009-002). We would like to thank the editor-in-chief and anonymous reviewers for their constructive comments, which substantially improved our manuscript.

ABBREVIATIONS

REE, rare earth elements; REY, lanthanides and yttrium; REO, oxides of REY-lanthanides and yttrium; CCBs, coal combustion byproducts; CCPs, coal combustion products; CMD, coal mine drainage; LTA, low-temperature ashing; XRD, X-ray diffraction analysis; SEM-EDX, scanning electron microscope-energy spectrum analysis

REFERENCES

(1) Rode, M.; Suhr, U. Uncertainties in selected river water quality data. *Hydrol. Earth Syst. Sci.* **2007**, *11*, 863−874.

(2) Dutta, T.; Kim, K.-H.; Uchimiya, M.; Kwon, E. E.; Jeon, B.-H.; Deep, A.; Yun, S.-T. Global demand for rare earth resources and strategies for green mining. *Environ. Res.* **2016**, *150*, 182−190.

(3) Valentim, B.; Abagiu, A. T.; Anghelescu, L.; Flores, D.; French, D.; Gonçalves, P.; Guedes, A.; Popescu, L. G.; Predeanu, G.; Ribeiro, J.; et al. Assessment of bottom ash landfilled at Ceplea Valley (Romania) as a source of rare earth elements. *Int. J. Coal Geol.* **2019**, *201*, 109−126.

(4) U.S. Geological Survey. *Mineral Commodity Summaries 2023*; U.S. Geological Survey, 2023.

(5) Xie, K.; Li, W.; Zhao, W. Coal chemical industry and its sustainable development in China. *Energy* **2010**, *35* (11), 4349−4355.

(6) Lin, R.; Soong, Y.; Granite, E. J. Evaluation of trace elements in U.S. coals using the USGS COALQUAL database version 3.0. Part I: Rare earth elements and yttrium (REY). *Int. J. Coal Geol.* **2018**, *192*, 1−13.

(7) Gagarin, H.; Sridhar, S.; Lange, I.; Bazilian, M. D. Considering non-power generation uses of coal in the United States. *Renew. Sustain. Energy Rev.* **2020**, *124*, 109790.

(8) Dai, S.; Ren, D.; Chou, C.-L.; Finkelman, R. B.; Seredin, V. V.; Zhou, Y. Geochemistry of trace elements in Chinese coals: A review of abundances, genetic types, impacts on human health, and industrial utilization. *Int. J. Coal Geol.* **2012**, *94*, 3−21.

(9) Dai, S.; Graham, I. T.; Ward, C. R. A review of anomalous rare earth elements and yttrium in coal. *Int. J. Coal Geol.* **2016**, *159*, 82−95.

(10) Seredin, V. V.; Dai, S. Coal deposits as potential alternative sources for lanthanides and yttrium. *Int. J. Coal Geol.* **2012**, *94*, 67−93.

(11) Hower, J. C.; Groppo, J. G.; Henke, K. R.; Hood, M. M.; Eble, C. F.; Honaker, R. Q.; Zhang, W.; Qian, D. Notes on the Potential for

the Concentration of Rare Earth Elements and Yttrium in Coal Combustion Fly Ash. *Minerals* **2015**, *5* (2), 356−366.
(12) Hower, J. C.; Granite, E. J.; Mayfield, D. B.; Lewis, A. S.; Finkelman, R. B. Notes on Contributions to the Science of Rare Earth Element Enrichment in Coal and Coal Combustion Byproducts. *Minerals* **2016**, *6* (2), 32.
(13) Dai, S.; Jiang, Y.; Ward, C. R.; Gu, L.; Seredin, V. V.; Liu, H.; Zhou, D.; Wang, X.; Sun, Y.; Zou, J.; Ren, D. Mineralogical and geochemical compositions of the coal in the Guanbanwusu Mine, Inner Mongolia, China: Further evidence for the existence of an Al (Ga and REE) ore deposit in the Jungar Coalfield. *Int. J. Coal Geol.* **2012**, *98*, 10−40.
(14) Taggart, R. K.; Hower, J. C.; Dwyer, G. S.; Hsu-Kim, H. Trends in the Rare Earth Element Content of U.S.-Based Coal Combustion Fly Ashes. *Environ. Sci. Technol.* **2016**, *50* (11), 5919−5926.
(15) Finkelman, R. B.; Wolfe, A.; Hendryx, M. S. The future environmental and health impacts of coal. *Energy Geosci.* **2021**, *2* (2), 99−112.
(16) Pan, J.; Nie, T.; Zhou, C.; Yang, F.; Jia, R.; Zhang, L.; Liu, H. The effect of calcination on the occurrence and leaching of rare earth elements in coal refuse. *J. Environ. Chem. Eng.* **2022**, *10* (5), 108355.
(17) Seredin, V. V.; Finkelman, R. B. Metalliferous coals: A review of the main genetic and geochemical types. *Int. J. Coal Geol.* **2008**, *76* (4), 253−289.
(18) Dai, S.; Yan, X.; Ward, C. R.; Hower, J. C.; Zhao, L.; Wang, X.; Zhao, L.; Ren, D.; Finkelman, R. B. Valuable elements in Chinese coals: A review. *Coal Geology of China*; Routledge, 2020; pp 60−90.
(19) Dai, S.; Zheng, X.; Wang, X.; Finkelman, R. B.; Jiang, Y.; Ren, D.; Yan, X.; Zhou, Y. Stone coal in China: A review. *Coal Geology of China*; Routledge, 2020; pp 206−223.
(20) Montross, S. N.; Verba, C. A.; Chan, H. L.; Lopano, C. Advanced characterization of rare earth element minerals in coal utilization byproducts using multimodal image analysis. *Int. J. Coal Geol.* **2018**, *195*, 362−372.
(21) Chen, H.; Zhang, L.; Pan, J.; Long, X.; He, X.; Zhou, C. Study on modes of occurrence and enhanced leaching of critical metals (lithium, niobium, and rare earth elements) in coal gangue. *J. Environ. Chem. Eng.* **2022**, *10* (6), 108818.
(22) Zhao, F.; Cong, Z.; Sun, H.; Ren, D. The geochemistry of rare earth elements (REE) in acid mine drainage from the Sitai coal mine, Shanxi Province, North China. *Int. J. Coal Geol.* **2007**, *70* (1−3), 184−192.
(23) Grawunder, A.; Merten, D.; Büchel, G. Origin of middle rare earth element enrichment in acid mine drainage-impacted areas. *Environ. Sci. Pollut. Res.* **2014**, *21* (11), 6812−6823.
(24) Ayora, C.; Macías, F.; Torres, E.; Lozano, A.; Carrero, S.; Nieto, J.-M.; Pérez-López, R.; Fernández-Martínez, A.; Castillo-Michel, H. Recovery of Rare Earth Elements and Yttrium from Passive-Remediation Systems of Acid Mine Drainage. *Environ. Sci. Technol.* **2016**, *50* (15), 8255−8262.
(25) Stewart, B. W.; Capo, R. C.; Hedin, B. C.; Hedin, R. S. Rare earth element resources in coal mine drainage and treatment precipitates in the Appalachian Basin, USA. *Int. J. Coal Geol.* **2017**, *169*, 28−39.
(26) Dai, S.; Zhao, L.; Hower, J. C.; Johnston, M. N.; Song, W.; Wang, P.; Zhang, S. Petrology, Mineralogy, and Chemistry of Size-Fractioned Fly Ash from the Jungar Power Plant, Inner Mongolia, China, with Emphasis on the Distribution of Rare Earth Elements. *Energy Fuels* **2014**, *28* (2), 1502−1514.
(27) Kolker, A.; Scott, C.; Hower, J. C.; Vazquez, J. A.; Lopano, C. L.; Dai, S. Distribution of rare earth elements in coal combustion fly ash, determined by SHRIMP-RG ion microprobe. *Int. J. Coal Geol.* **2017**, *184*, 1−10.
(28) Lefticariu, L.; Klitzing, K. L.; Kolker, A. Rare Earth Elements and Yttrium (REY) in coal mine drainage from the Illinois Basin, USA. *Int. J. Coal Geol.* **2020**, *217*, 103327.
(29) Hao, H.; Li, J.; Wang, J.; Liu, Y.; Sun, Y. Distribution characteristics and enrichment model of valuable elements in coal: An example from the Nangou Mine, Ningwu Coalfield, northern China. *Ore Geol. Rev.* **2023**, *160*, 105599.
(30) Zhao, L.; Dai, S.; Nechaev, V. P.; Nechaeva, E. V.; Graham, I. T.; French, D.; Sun, J. Enrichment of critical elements (Nb-Ta-Zr-Hf-REE) within coal and host rocks from the Datanhao mine, Daqingshan Coalfield, northern China. *Ore Geol. Rev.* **2019**, *111*, 102951.
(31) Hussain, R.; Luo, K. Geochemical Evaluation of Enrichment of Rare-Earth and Critical Elements in Coal Wastes from Jurassic and Permo-Carboniferous Coals in Ordos Basin, China. *Nat. Resour. Res.* **2020**, *29* (3), 1731−1754.
(32) Dai, S.; Li, D.; Chou, C.-L.; Zhao, L.; Zhang, Y.; Ren, D.; Ma, Y.; Sun, Y. Mineralogy and geochemistry of boehmite-rich coals: New insights from the Haerwusu Surface Mine, Jungar Coalfield, Inner Mongolia, China. *Int. J. Coal Geol.* **2008**, *74* (3−4), 185−202.
(33) Lin, R.; Howard, B. H.; Roth, E. A.; Bank, T. L.; Granite, E. J.; Soong, Y. Enrichment of rare earth elements from coal and coal by-products by physical separations. *Fuel* **2017**, *200*, 506−520.
(34) Ziemkiewicz, P. *Recovery of Rare Earth Elements (REEs) from Coal Mine Drainage, Phase 2*; West Virginia Univ.: Morgantown, WV (United States), 2020.
(35) Finkelman, R. B. Trace and Minor Elements in Coal. In *Organic Geochemistry: Principles and Applications*; Engel, M. H., Macko, S. A., Eds.; Vol. *11*; Springer US, 1993; pp 593−607.
(36) Zhao, Z. G.; Tang, X. Y. Rare-earth elements in coal of China. *Coal Geol. China* **2002**, *14*, 70−74.
(37) Zhang, W.; Rezaee, M.; Bhagavatula, A.; Li, Y.; Groppo, J.; Honaker, R. A review of the occurrence and promising recovery methods of rare earth elements from coal and coal by-products. *Int. J. Coal Prep. Util.* **2015**, *35* (6), 295−330.
(38) Taylor, S. R.; McLennan, S. M. *Continental Crust: its Composition and Evolution. An Examination of the Geochemical Record Preserved in Sedimentary Rocks*; Blackwell Scientific, 1985.
(39) Huanjie, L.; Yuru, J.; Yaozhen, L.; Hongwei, W. Study on lithofacies paleogeography of Zhungeer coal field and its methodology in Inner Mongolia of China. *Int. J. Coal Geol.* **1990**, *16* (1−3), 181−183.
(40) Zhao, Q.; Sun, B.; Li, W. Formation Condition and Exploration Target of Large Coalbed Methane Gas Field in Eastern Ordos Basin. In *Petroleum Exploration and Development*; KeAi, 1998; pp 20−23.
(41) ASTM *Standard Practice for Preparing Coal Samples for Microscopical Analysis by Reflected Light*; ASTM International: West Conshohocken, PA, USA, 2011.
(42) Ward, C. R. Analysis and significance of mineral matter in coal seams. *Int. J. Coal Geol.* **2002**, *50* (1−4), 135−168.
(43) Speight, J. G. Mineral Matter. *Handbook of Coal Analysis*; John Wiley & Sons, 2015; pp 84−115.
(44) Dai, S.; Liu, J.; Ward, C. R.; Hower, J. C.; French, D.; Jia, S.; Hood, M. M.; Garrison, T. M. Mineralogical and geochemical compositions of Late Permian coals and host rocks from the Guxu Coalfield, Sichuan Province, China, with emphasis on enrichment of rare metals. *Int. J. Coal Geol.* **2016**, *166*, 71−95.
(45) Ketris, M. á.; Yudovich, Y. E. Estimations of Clarkes for Carbonaceous biolithes: World averages for trace element contents in black shales and coals. *Int. J. Coal Geol.* **2009**, *78* (2), 135−148.
(46) Guo, X.; Tang, Y.; Wang, Y.; Eble, C. F.; Finkelman, R. B.; Huan, B.; Pan, X. Potential utilization of coal gasification residues from entrained-flow gasification plants based on rare earth geochemical characteristics. *J. Clean. Prod.* **2021**, *280*, 124329.
(47) Johannesson, K. H.; Xiaoping, Z. Geochemistry of the rare earth elements in natural terrestrial waters: A review of what is currently known. *Chin. J. Geochem.* **1997**, *16* (1), 20−42.
(48) Wenming, D.; Hongxia, Z.; Meide, H.; Zuyi, T. Use of the ion exchange method for the determination of stability constants of trivalent metal complexes with humic and fulvic acids—Part I: Eu3+ and Am3+ complexes in weakly acidic conditions. *Appl. Radiat. Isot.* **2002**, *56* (6), 959−965.
(49) Zhou, J.; Zhuang, X.; Alastuey, A.; Querol, X.; Li, J. Geochemistry and mineralogy of coal in the recently explored

https://doi.org/10.1021/acsomega.4c00546
ACS Omega 2024, 9, 32481−32501

Zhundong large coal field in the Junggar basin, Xinjiang province, China. *Int. J. Coal Geol.* **2010**, *82* (1−2), 51−67.
(50) Seredin, V. V. Rare earth element-bearing coals from the Russian Far East deposits. *Int. J. Coal Geol.* **1996**, *30* (1−2), 101−129.
(51) Dai, S.; Wang, X.; Zhou, Y.; Hower, J. C.; Li, D.; Chen, W.; Zhu, X.; Zou, J. Chemical and mineralogical compositions of silicic, mafic, and alkali tonsteins in the late Permian coals from the Songzao Coalfield, Chongqing, Southwest China. *Chem. Geol.* **2011**, *282* (1−2), 29−44.
(52) Li, G.; Guo, Y.; Wang, H.; Li, M.; Han, J.; Yang, X. Sedimentology and Paleoenvironmental Characteristics of Fine-grained Sediments in Coal-bearing Strata in the Eastern Ordos Basin: A Case Study of the Exploratory Well in the Zizhou Area. *Acta Geol. Sin.* **2023**, *97* (4), 1181−1195.
(53) Yu, C.; Mu, N.; Huang, W.; Xu, W.; Feng, X. Major and Rare Earth Element Characteristics of Late Paleozoic Coal in the Southeastern Qinshui Basin: Implications for Depositional Environments and Provenance. *ACS Omega* **2022**, *7* (35), 30856−30878.
(54) Jiu, B.; Huang, W.; Mu, N. Mineralogy and elemental geochemistry of Permo-Carboniferous Li-enriched coal in the southern Ordos Basin, China: Implications for modes of occurrence, controlling factors and sources of Li in coal. *Ore Geol. Rev.* **2022**, *141*, 104686.
(55) Dai, S.; Finkelman, R. B. Coal as a promising source of critical elements: Progress and future prospects. *Int. J. Coal Geol.* **2018**, *186*, 155−164.
(56) Nechaev, V. P.; Chekryzhov, I. Y.; Vysotskiy, S. V.; Ignatiev, A. V.; Velivetskaya, T. A.; Tarasenko, I. A.; Agoshkov, A. I. Isotopic signatures of REY mineralization associated with lignite basins in South Primorye, Russian Far East. *Ore Geol. Rev.* **2018**, *103*, 68−77.
(57) Abedini, A.; Calagari, A. A.; Azizi, M. R. The tetrad-effect in rare earth elements distribution patterns of titanium-rich bauxites: Evidence from the Kanigorgeh deposit, NW Iran. *J. Geochem. Explor.* **2018**, *186*, 129−142.
(58) Maksimovic, Z.; Pantó, G. Contribution to the geochemistry of the rare earth elements in the karst-bauxite deposits of Yugoslavia and Greece. *Geoderma* **1991**, *51* (1−4), 93−109.
(59) Dai, S.; Luo, Y.; Seredin, V. V.; Ward, C. R.; Hower, J. C.; Zhao, L.; Liu, S.; Zhao, C.; Tian, H.; Zou, J. Revisiting the late Permian coal from the Huayingshan, Sichuan, southwestern China: Enrichment and occurrence modes of minerals and trace elements. *Int. J. Coal Geol.* **2014**, *122*, 110−128.
(60) Gray, A. L.; Williams, J. G. Communication. Oxide and doubly charged ion response of a commercial inductively coupled plasma mass spectrometry instrument. *J. Anal. At. Spectrom.* **1987**, *2* (1), 81−82.
(61) Raut, N. M.; Huang, L.-S.; Aggarwal, S. K.; Lin, K.-C. Determination of lanthanides in rock samples by inductively coupled plasma mass spectrometry using thorium as oxide and hydroxide correction standard. *Spectrochim. Acta, Part B* **2003**, *58* (5), 809−822.
(62) Zhou, T.; Wu, C.; Yuan, B.; Shi, Z.; Wang, J.; Zhu, W.; Zhou, Y.; Jiang, X.; Zhao, J.; Wang, J.; Ma, J. New insights into multiple provenances evolution of the Jurassic from heavy minerals characteristics in southern Junggar Basin, NW China. *Petrol. Explor. Dev.* **2019**, *46* (1), 67−81.
(63) Jiu, B.; Huang, W.; Hao, R. A method for judging depositional environment of coal reservoir based on coal facies parameters and rare earth element parameters. *J. Pet. Sci. Eng.* **2021**, *207*, 109128.
(64) Hower, J. C.; Ruppert, L. F.; Eble, C. F. Lanthanide, yttrium, and zirconium anomalies in the Fire Clay coal bed, Eastern Kentucky. *Int. J. Coal Geol.* **1999**, *39* (1−3), 141−153.
(65) Dai, S.; Ren, D.; Li, S. Modes of Occurrence of Rare Earth Elements in Some Late Paleozoic Coals of North China. *Acta Geosci. Sin.* **2003**, *24* (03), 273−278.
(66) Dai, S.; Zhang, W.; Ward, C. R.; Seredin, V. V.; Hower, J. C.; Li, X.; Song, W.; Wang, X.; Kang, H.; Zheng, L.; et al. Mineralogical and geochemical anomalies of late Permian coals from the Fusui Coalfield, Guangxi Province, southern China: Influences of terrigenous materials and hydrothermal fluids. *Int. J. Coal Geol.* **2013**, *105*, 60−84.
(67) Berry, W. B.; Wilde, P. Progressive ventilation of the oceans; an explanation for the distribution of the lower Paleozoic black shales. *Am. J. Sci.* **1978**, *278* (3), 257−275.
(68) Chen, Z. H.; Du, J. Y.; Lu, S.; Ma, R. Z.; Wang, X. T. Study on rare earth export price index based on export statistics. *Chin. Rare Earths* **2015**, *36* (3), 131−134.
(69) Dai, S.; Ren, D.; Chou, C. L.; Li, S.; Jiang, Y. Mineralogy and geochemistry of the No. 6 Coal (Pennsylvanian) in the Junger Coalfield, Ordos Basin, China. *Int. J. Coal Geol.* **2006**, *66* (4), 253−270.
(70) Liu, Y. *Introduction to Element Geochemistry*; Geological Publishing House, 1987.
(71) Lu, Z.; Liu, C.-q.; Liu, J.-j.; Wu, F.-c. Geochemical studies on the Lower Cambrian witherite-bearing cherts in the northern Daba Mountains. *Acta Geol. Sin.* **2004**, *78* (3), 390−406.
(72) Dai, S.; Hower, J. C.; Finkelman, R. B.; Graham, I. T.; French, D.; Ward, C. R.; Eskenazy, G.; Wei, Q.; Zhao, L. Organic associations of non-mineral elements in coal: A review. *Int. J. Coal Geol.* **2020**, *218*, 103347.
(73) Finkelman, R. B.; Dai, S.; French, D. The importance of minerals in coal as the hosts of chemical elements: A review. *Int. J. Coal Geol.* **2019**, *212*, 103251.
(74) Eskenazy, G. M. Rare earth elements in a sampled coal from the Pirin deposit, Bulgaria. *Int. J. Coal Geol.* **1987**, *7* (3), 301−314.
(75) Finkelman, R. B. Modes of occurrence of potentially hazardous elements in coal: levels of confidence. *Fuel Process. Technol.* **1994**, *39* (1−3), 21−34.
(76) Moldoveanu, G. A.; Papangelakis, V. G. An overview of rare-earth recovery by ion-exchange leaching from ion-adsorption clays of various origins. *Mineral. Mag.* **2016**, *80* (1), 63−76.
(77) Chen, L.; Jin, X.; Chen, H.; He, Z.; Qiu, L.; Duan, H. Grain Size Distribution and Clay Mineral Distinction of Rare Earth Ore through Different Methods. *Minerals* **2020**, *10* (4), 353.
(78) Sobri, N. A.; Yunus, M. Y. B. M.; Harun, N. A review of ion adsorption clay as a high potential source of rare earth minerals in Malaysia. In *Materials Today: Proceedings*; Elsevier, 2023.
(79) Jin, X.; Chen, L.; Chen, H.; Zhang, L.; Wang, W.; Ji, H.; Deng, S.; Jiang, L. XRD and TEM analyses of a simulated leached rare earth ore deposit: Implications for clay mineral contents and structural evolution. *Ecotoxicol. Environ. Saf.* **2021**, *225*, 112728.
(80) Dai, S.; Finkelman, R. B.; French, D.; Hower, J. C.; Graham, I. T.; Zhao, F. Modes of occurrence of elements in coal: A critical evaluation. *Earth-Sci. Rev.* **2021**, *222*, 103815.
(81) Cheng, W.; Zhang, Q.; Yang, R.; Tian, Y. Occurrence modes and cleaning potential of sulfur and some trace elements in a high-sulfur coal from Pu'an coalfield, SW Guizhou, China. *Environ. Earth Sci.* **2014**, *72* (1), 35−46.
(82) Dai, S.; Zou, J.; Jiang, Y.; Ward, C. R.; Wang, X.; Li, T.; Xue, W.; Liu, S.; Tian, H.; Sun, X.; Zhou, D. Mineralogical and geochemical compositions of the Pennsylvanian coal in the Adaohai Mine, Daqingshan Coalfield, Inner Mongolia, China: Modes of occurrence and origin of diaspore, gorceixite, and ammonian Illite. *Int. J. Coal Geol.* **2012**, *94*, 250−270.
(83) Kang, J.; Zhao, L.; Wang, X.; Song, W.; Wang, P.; Wang, R.; Li, T.; Sun, J.; Jia, S.; Zhu, Q. Abundance and geological implication of rare earth elements and yttrium in coals from the Suhaitu Mine, Wuda Coalfield, northern China. *Energy Explor. Exploit.* **2014**, *32* (5), 873−889.
(84) Huang, W.; Yang, Q.; Tang, D.; Tang, X.; Zhao, Z. Rare earth element geochemistry of Late Palaeozoic coals in North China. *Acta Geol. Sin.* **2000**, *74* (1), 74−83.
(85) Finkelman, R. B. Modes of Occurrence of Environmentally-Sensitive Trace Elements in Coal. In *Environmental Aspects of Trace Elements in Coal*; Swaine, D. J., Goodarzi, F., Eds.; Springer Netherlands, 1995; pp 24−50.
(86) Qin, S.; Gao, K.; Sun, Y.; Wang, J.; Zhao, C.; Li, S.; Lu, Q. Geochemical Characteristics of Rare-Metal, Rare-Scattered, and Rare-

https://doi.org/10.1021/acsomega.4c00546
ACS Omega 2024, 9, 32481−32501

Earth Elements and Minerals in the Late Permian Coals from the Moxinpo Mine, Chongqing, China. *Energy Fuels* **2018**, *32* (3), 3138−3151.
(87) Wang, X.; Dai, S.; Sun, Y.; Li, D.; Zhang, W.; Zhang, Y.; Luo, Y. Modes of occurrence of fluorine in the Late Paleozoic No. 6 coal from the Haerwusu Surface Mine, Inner Mongolia, China. *Fuel* **2011**, *90* (1), 248−254.
(88) Sun, Y.; Zhao, C.; Li, Y.-H.; Wang, J.-X. Minimum mining grade of the selected trace elements in Chinese coal. *J. China Coal Soc.* **2014**, *39* (04), 744−748.
(89) Nechaev, V. P.; Dai, S.; Chekryzhov, I. Y.; Tarasenko, I. A.; Zin'kov, A. V.; Moore, T. A. Origin of the tuff parting and associated enrichments of Zr, REY, redox-sensitive and other elements in the Early Miocene coal of the Siniy Utyes Basin, southwestern Primorye, Russia. *Int. J. Coal Geol.* **2022**, *250*, 103913.
(90) Sutcu, E. C.; Şentürk, S.; Kapıcı, K.; Gökçe, N. Mineral and rare earth element distribution in the Tunçbilek coal seam, Kütahya, Turkey. *Int. J. Coal Geol.* **2021**, *245*, 103820.
(91) Crowley, S. S.; Stanton, R. W.; Ryer, T. A. The effects of volcanic ash on the maceral and chemical composition of the C coal bed, Emery Coal Field, Utah. *Org. Geochem.* **1989**, *14* (3), 315−331.
(92) Shi, S.; Liu, Q.; Sun, J.; Wu, Z.; Sun, B. Enrichment features and causes of boehmite in high-alumina partings of Junger coalfield. *Coal Eng.* **2014**, *46* (5), 116−118.
(93) Wen, L.; Huang, W.; Zhang, Y.; Jiu, B. Geochemical characteristics of rare earth elements in late Palaeozoic coals from North China. *Front. Earth Sci.* **2024**, *12*, 1374780.
(94) Zhao, Z.; Tang, X.; Li, B. Geochemistry of rare-earth elements of coal in Huainan mining area. *Acta Sedimentol. Sin.* **2000**, *18* (3), 453−459.
(95) Li, H.; Hao, y.; Yang, L.; Liu, Y. Characteristics of Bitumen Trace Elements and Rare Earth Elements of Coal in Southeastern Margin of Ordos Basin. *Xinjiang Pet. Geol.* **2008**, *2*, 159−162.
(96) Liu, D.; Yang, Q.; Tang, D. Occurrence and Geological Genesis of Pyritesin Late Paleozoic Coals in North China. *Chin. J. Geochem.* **2000**, *19* (04), 301−311.
(97) Huang, W.; Yang, Q.; Peng, S.; Zhao, Z. Geochemistry of Permian Coal and Its Combustion Residues in Huainan Coalfield, China. *J. Earth Sci.* **2001**, *12* (04), 283−290.
(98) Senesi, N.; Adriano, D. C. *Metal-Humic Substance Complexes in the Environment. Molecular and Mechanistic Aspects by Multiple Spectroscopic Approach*; Taylor & Francis Group, 1991.
(99) Eskenazy, G. M. Aspects of the geochemistry of rare earth elements in coal: an experimental approach. *Int. J. Coal Geol.* **1999**, *38* (3−4), 285−295.
(100) Zhang, H.-F. *Temporal and Spatial Distribution of Mesozoic Mafic Magmatism in the North China Craton and Implications for Secular Lithospheric Evolution*; Geological Society, London, Special Publications 2007; Vol. *280*(1), pp 35−54.
(101) Allègre, C. J.; Minster, J. F. Quantitative models of trace element behavior in magmatic processes. *Earth Planet. Sci. Lett.* **1978**, *38* (1), 1−25.

https://doi.org/10.1021/acsomega.4c00546
ACS Omega 2024, 9, 32481−32501